Intensity discrimination as a function of stimulus level with electric stimulation

David A. Nelson, Jennifer L. Schmitz, Gail S. Donaldson, Neal F. Viemeister, and Eric Javel
Clinical Psychoacoustics Laboratory, University of Minnesota, Minneapolis, Minnesota 55455

(Received 31 July 1995; revised 30 April 1996; accepted 8 May 1996)

Difference limens (DLs) for changes in electric current were measured from multiple electrodes in each of eight cochlear-implanted subjects. Stimuli were 200-μs/phase biphasic pulse trains delivered at 125 Hz in 300-ms bursts. DLs were measured with an adaptive three-alternative forced-choice procedure. Fixed-level psychometric functions were also obtained in four subjects to validate the adaptive DLs. Relative intensity DLs, specified as Weber fractions in decibels $\{10 \log(\Delta I/I)\}$ for standards above absolute threshold, decreased as a power function of stimulus intensity relative to absolute threshold $\{\Delta I/I = \beta(I/I_0)^{\alpha}\}$ in the same manner as Weber fractions for normal acoustic stimulation reported in previous studies. Exponents (α) of the power function for electric stimulation ranged from -0.4 to -3.2, on average, an order of magnitude larger than exponents for acoustic stimulation, which range from -0.07 to -0.11. Normalization of stimulus intensity to the dynamic range of hearing resulted in Weber functions with similar negative slopes for electric and acoustic stimulation, corresponding to an 8-dB average improvement in Weber fractions across the dynamic range. Sensitivity to intensity change $\{10 \log \beta\}$ varied from -0.42 to -13.5 dB compared to $+0.60$ to -3.34 dB for acoustic stimulation, but on average was better with electric stimulation than with acoustic stimulation. Psychometric functions for intensity discrimination yielded Weber fractions consistent with adaptive procedures and d' was a linear function of ΔI. Variability among repeated Weber-fraction estimates was constant across dynamic range. Relatively constant Weber fractions across all or part of the dynamic range, observed in some subjects, were traced to the intensity resolution limits of individual implanted receiver/stimulators. DLs could not be accurately described by constant amplitude changes, expressed as a percentage of dynamic range $\{\Delta A(\%\mathrm{DR})\}$. Weber fractions from prelingually deafened subjects were no better or worse than those from postlingually deafened subjects. The cumulative number of discriminable intensity steps across the dynamic range of electric hearing ranged from as few as 6.6 to as many as 45.2. Physiologic factors that may determine important features of electric intensity discrimination are discussed in the context of a simple, qualitative, rate-based model. These factors include the lack of compressive cochlear preprocessing, the relative steepness of neural rate-intensity functions, and individual differences in patterns of neural survival.

PACS numbers: 43.66.Ts, 43.66.Sr, 43.66.Cb, 43.64.Me [LLF]

INTRODUCTION

The ability of deafened listeners to discriminate small changes in electric current is a fundamental consideration with respect to the design of implantable cochlear prostheses. Previous studies suggest that intensity discrimination for electric stimulation of the cochlea is sometimes better and sometimes worse than it is for acoustic stimulation (Simmons, 1966; Douek *et al.*, 1977; Eddington *et al.*, 1978; Fourcin *et al.*, 1979; Aran, 1981; Hochmair-Desoyer *et al.*, 1981; House and Edgerton, 1982; Hochmair-Desoyer *et al.*, 1983; Tong *et al.*, 1988), depending upon the psychophysical method used to collect the data, the particular stimulus waveform used, and the level at which intensity discrimination is measured. For a complete review, see the reports by Pfingst and co-workers (1983, 1984, 1988).

Only a few studies have investigated intensity discrimination across the entire dynamic range of electric hearing. Pfingst and co-workers (Pfingst *et al.*, 1983; Pfingst, 1984; Pfingst and Rai, 1990) evaluated relative intensity difference limens (DLs) in monkeys using primarily sinusoidal electric stimulation, and reported a consistent improvement in the DL with stimulus level. They also reported that electric DLs were somewhat poorer than acoustic DLs in monkeys. Shannon (1983) described electric DLs for a single human subject using 100- and 1000-Hz sinusoids and different electrode configurations. DLs improved with stimulus level and were slightly better than acoustic DLs. Hochmair-Desoyer *et al.* (1981), using 300-Hz sinusoids in a single subject, reported electric DLs that were an order of magnitude smaller than acoustic DLs, but improved only slightly with stimulus level. Dillier *et al.* (1983), using 100-Hz biphasic pulses, also reported electric DLs that were an order of magnitude better than acoustic DLs. One of their subjects improved with stimulus level but the other did not. These studies involve too few subjects and too few stimulus conditions to adequately address questions of mechanisms underlying intensity discrimination or to evaluate the significance of intersubject variability. Furthermore, data are sparse for bipolar

TABLE I. Subject code, age at implant surgery, insertion depth of electrode array (mm from round window), number of years of deafness before surgery, and primary cause of deafness.

Subject	Age	Depth	Yrs deaf	Primary cause of deafness
JWB	51	20	4	Cochlear otosclerosis
TVB	41	22	8	Progressive snhl
DVS	44	22	10	Congenital; progressive snhl
RFM	57	22	1	Meniere's disease
JPB	52	24	4	Hereditary; progressive snhl
EES	54	17	4	Cogan's syndrome
FXC	64	25	4	Noise-induced; progressive snhl
AMA	58	19	58	Congenital

pulsatile stimuli, even though such stimuli are in widespread clinical use.

The present research evaluates relative intensity DLs, or Weber fractions, as a function of stimulus level, using bipolar pulsatile stimuli. It was undertaken to address several general issues: First, given the wide range of electric DLs reported by previous studies, using a variety of psychophysical methods and stimulation schemes, we wanted to determine whether such large differences could be demonstrated, either across subjects or across electrodes in a particular subject, when psychophysical method and stimulation scheme were held constant. If large differences do exist, then they may stem from local differences in absolute threshold and dynamic range along the electrode array, which, in turn, may reflect characteristics of the surviving neural population. Furthermore, such differences may contribute significantly to differences in subjects' speech recognition performance. Second, we wanted to determine how Weber fractions change across the dynamic range, so that comparisons could be made to acoustic Weber fractions in normal-hearing listeners. In acoustic listeners, Weber fractions for tones improve consistently with increasing sensation level (Jesteadt *et al.*, 1977), presumably reflecting the nonlinear spread of excitation that occurs with stimulus level in the cochlea. For a thorough review of intensity discrimination with acoustic stimulation in humans see Viemeister (1988). Since nonlinear excitation patterns are not present in electric stimulation, comparisons of electric and acoustic Weber fractions may provide clues to the theoretical mechanisms underlying intensity discrimination. Finally, a more definitive knowledge of Weber fractions in individual implant subjects is needed to evaluate the appropriateness of various compression schemes used in the design and fitting of cochlear implant processors.

I. METHODS

A. Subjects

Subjects were seven postlingually deafened adults and one prelingually deafened adult (AMA) who had been implanted with a Nucleus 22-electrode device. Table I displays the age of each subject at the time of implantation, depth of insertion of the electrode array, the number of years each subject was deaf before implant surgery, and the primary cause of deafness. All subjects were experienced implant users, having used their devices for 4 to 7 years prior to participating in this study. For most subjects, electric stimulation was bipolar between every other electrode (BP+1), which corresponds to a spatial extent of 1.5 mm between electrode pairs. For two subjects, electric stimulation was bipolar between adjacent electrodes, which corresponds to a spatial extent of 0.75 mm. In this report, electrodes are numbered from 01 to 22, starting at the apical end of the electrode array.[1] Electrode pairs are specified by the more basal member.

For four subjects, Weber fractions were measured on six electrodes across the electrode array. One electrode near the basal end, one electrode near the apical end, and four additional adjacent electrodes that demonstrated disparate dynamic ranges, were chosen for testing. In cases where only a limited number of electrodes was available, due to suboptimal insertion depth or undesirable percepts (e.g., facial nerve stimulation), the most basal or apical electrodes available were tested. In the remaining four subjects, three electrodes were selected for testing, one each in the apical, middle and basal regions of the implanted array. Table II lists the bipolar separation and electrode pairs used with each subject.

B. Stimuli

Experiments were controlled by a 12-MHz 80286 AT computer connected through a parallel port to a BTNl cochlear implant interface (Shannon *et al.*, 1990). The interface allowed computer control of the Nucleus receiver/stimulator. Stimuli used in this study were either 500- or 300-ms pulse trains comprised of 200-μs/phase biphasic current pulses presented at a rate of 125 pulses/s.

TABLE II. Subject codes, stimulation scheme and electrode pairs tested. Stimulation modes used were bipolar (BP) or bipolar+1 (BP+1), corresponding to spatial extents of 0.75 and 1.5 mm between electrode pairs. Electrode numbers increase from apex to base. Each electrode pair is referred to in the text by the higher-numbered (more basal) electrode.

Subject	Stimulation	Electrode pairs tested					
JWB	BP+1	07:05	11:09	12:10	13:11	14:12	17:15
TVB	BP	08:07	15:14	16:15	17:16	18:17	21:20
DVS	BP+1	06:04	09:07	10:08	11:09	12:10	19:17
RFM	BP+1	05:03	13:11	14:12	15:13	16:14	21:19
JPB	BP+1	07:05	11:09	16:14			
EES	BP+1	05:03	11:09	18:16			
FXC	BP+1	05:03	11:09	18:16			
AMA	BP	04:03	11:10	19:18			

C. Psychophysical procedures

1. Absolute thresholds and maximum acceptable loudness levels

Absolute detection thresholds and maximum acceptable loudness levels (MALs) were measured on all available electrodes of each subject's implanted array, using an ascending method of adjustment. Subjects were presented with 500-ms trains of biphasic pulses at a repetition rate of 1 train per s. The tester slowly increased stimulus level until the subject indicated that a sound was just audible (absolute threshold), then continued to increase current until MAL was reached. Absolute threshold and MAL estimates for three runs were averaged to obtain a single measure of each. Absolute thresholds and MALs were rechecked periodically to insure that there were no consistent changes during the course of the experiment.

Additional absolute threshold estimates were obtained to verify the initial method-of-adjustment absolute thresholds, using either a modified Bekesy tracking technique or a three-alternative forced-choice (3AFC) adaptive procedure. For the modified Bekesy tracking technique, 500-ms trains of biphasic pulses were initially presented 2 dB above the absolute threshold obtained with the adjustment procedure. Subjects were instructed to depress a mouse button as long as they heard a sound and to release it when the sound became inaudible. Stimulus level was slowly reduced in 0.5-dB steps until the subject released the button; stimulus level was then reduced another 2.0 dB and an ascending run was begun. This time, the level of the stimulus was increased in 0.5-dB steps until the subject pressed the button indicating that the sound was again audible. Stimulus level was then increased 2.0 dB and another descending run began. Alternating descending and ascending runs continued until 12 ''turn-arounds'' (levels at which the subject released or depressed the mouse button) were obtained. The mean value of the final eight turn-arounds was taken to be absolute threshold. An adaptive 3AFC threshold procedure estimated the current level corresponding to 79.4% correct detection using a three-down/one-up stepping rule. The same basic paradigm as in the adaptive intensity discrimination procedure was used (as described below), except that a 300-ms train of biphasic pulses was presented in only one of the three listening intervals. The subject's task was to detect which interval contained a sound. Absolute threshold determinations from three 3AFC tracks were averaged to obtain the final threshold estimate.

2. Adaptive Weber fractions

Weber fractions were obtained using a 3AFC adaptive procedure. Stimuli were 300-ms trains of 200-μs/phase biphasic pulses at 125 Hz, presented in three listening intervals. Two stimuli were presented at a fixed level (standard) and the third was presented at a higher level (comparison), with the comparison interval chosen at random on each trial. The subject's task was to decide which interval was ''loudest'' and respond by pressing the corresponding button on a three-button computer mouse. Stimulus intervals were cued by three sequentially lighted boxes on a video monitor. Correct answer feedback was provided after each trial. The comparison stimulus was initially 1–3 dB more intense than the standard stimulus. For the first four reversals, the comparison level was altered according to a one-down/one-up stepping rule, with step size equal to one-fourth of the initial difference (e.g., 2 dB/4=0.5 dB). These initial four reversals were intended to quickly move the adaptive procedure into the target region of discrimination threshold. After the fourth reversal, step size was reduced to one-eighth the initial difference (e.g., 2 dB/8=0.25 dB) and a three-down/one-up stepping rule was assumed. This stepping rule estimates the stimulus level corresponding to 79.4% correct discrimination (Levitt, 1971). Step size was constant for all remaining trials unless the decision rule called for the comparison stimulus to be presented at the level of the standard. If this occurred, the program moved from a fixed step size to a step size corresponding to a factor of 2 (e.g., 0.25/2=0.125 dB) until the level difference between the standard and the last presentation level again exceeded the previous fixed step size.

All stimulus levels presented during the 3AFC adaptive track were translated into the nearest realizable current step unit $(\mathrm{CSU})^2$ using a calibration table provided by Cochlear Corp. for each subject's implanted electrode array. On occasion, the adaptive stepping rule called for a level difference that, when translated into CSUs, corresponded to the same CSU for both the standard and the comparison intervals. If this occurred on five consecutive trials, the run was aborted and restarted. Trials continued until a total of 12 reversals occurred. The mean of the final eight reversals was taken as the DL estimate. The level difference at discrimination threshold was then converted to a Weber fraction in decibels.

Weber fractions were determined in this manner for four to seven intensity levels of the standard spanning the dynamic range of each electrode tested. Data were obtained in sets, where a single set was comprised of one adaptive track at each stimulus intensity, in increasing (low-to-high) order. In most cases, three or more sets were tested during a single listening session, which allowed any learning effects to be distributed across stimulus levels. Between each low-to-high level series, absolute threshold was retested to check for auditory fatigue effects. No obvious fatigue effects were observed. Sessions were repeated until at least three Weber fractions fell within a range of 5 dB at each stimulus level. In this report, we will use the term ''Weber function'' to refer to a set of Weber fractions obtained as a function of the level of the standard for a single electrode.

3. Psychometric functions for intensity discrimination

Psychometric functions for intensity discrimination, which define performance (in d' units) as a function of the size of the intensity change (ΔI), were evaluated in four subjects to confirm results obtained with the adaptive procedure. Stimuli were identical to those used in the adaptive procedure. A two-alternative forced-choice (2AFC) paradigm was used in which the standard and comparison stimuli were presented in random order and the subject was instructed to choose the interval with the louder signal. Ten

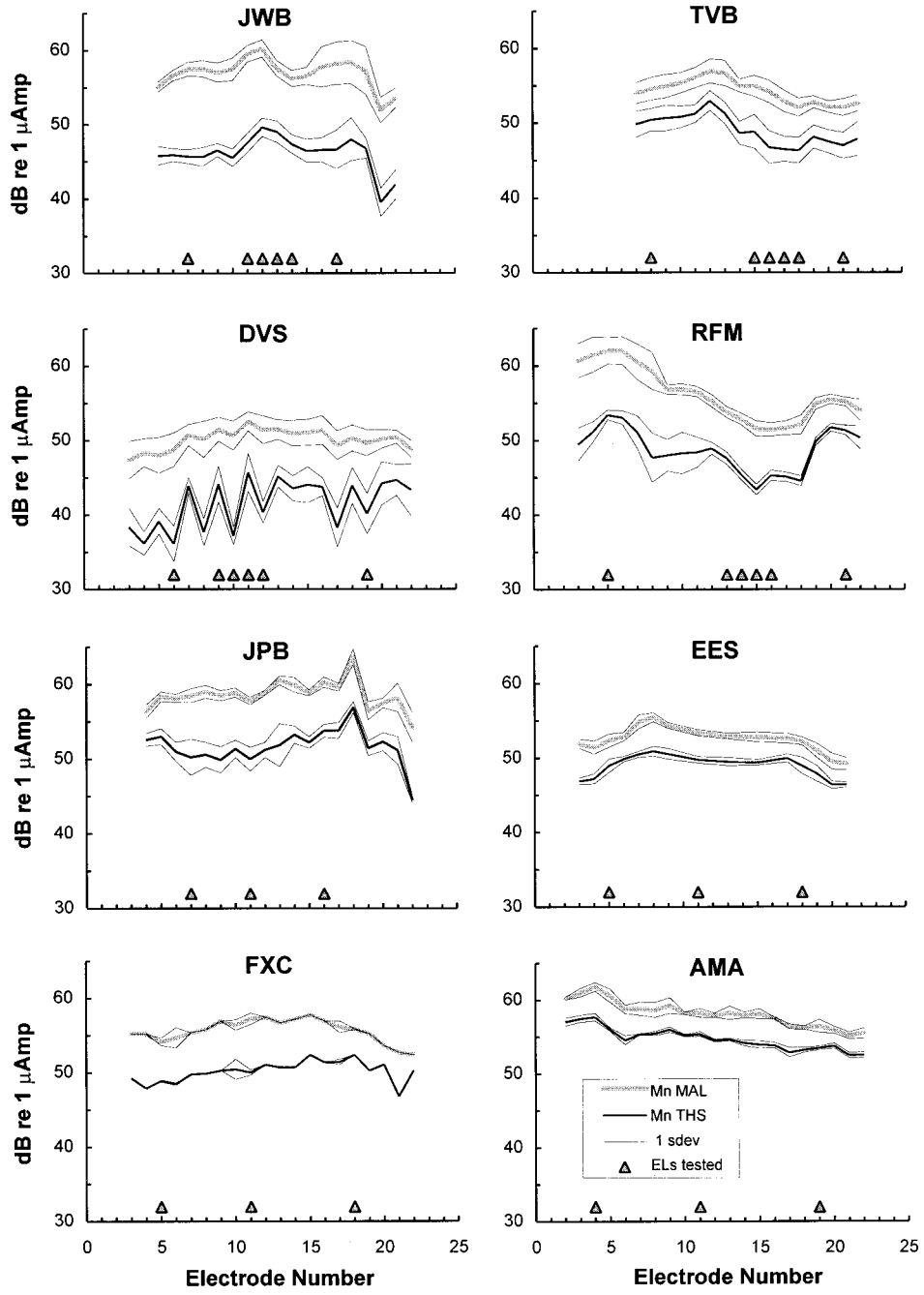

FIG. 1. Absolute thresholds and maximum acceptable loudness (MAL) levels for the eight subjects from whom Weber fractions were measured, plotted as a function of electrode number. Lower numbered electrodes are more apical along the electrode array. The upper curves in each panel show the average MALs (wide shaded curve) obtained over a series of test sessions, along with values one standard deviation above and below each average (thin curves). The lower curves in each panel indicate the average absolute threshold (wide dark curve) obtained over a series of test sessions, along with values one standard deviation above and below each average (thin curves). The electrodes for which Weber fractions were measured are indicated by the shaded triangles at the bottom of each panel.

levels of the comparison stimulus (usually consecutive CSUs) were tested for discrimination from the standard stimulus whenever possible. If the standard level was near the MAL and ten steps could not be tested, then the maximum number of steps available was used. Stimuli were presented in blocks of 20 trials. Each point in the psychometric function was based on four to five blocks, or a total of 80–100 trials per point.

II. RESULTS AND DISCUSSION

A. Absolute thresholds and maximum acceptable loudness levels

Figure 1 shows absolute thresholds and maximum acceptable loudness levels (MALs) for all usable electrodes in each subject's implanted electrode array. The top set of curves in each panel shows the mean MALs across elec-

trodes (wide shaded curve), together with values one standard deviation (s.d.) above and below the means. The bottom set of curves shows the mean absolute threshold obtained on each electrode (wide dark curve), along with ±1-s.d. values. Symbols (shaded triangles) along the bottom of each panel indicate those electrodes selected for intensity discrimination testing. Whenever possible, electrodes with widely different absolute thresholds were chosen.

The MALs for two subjects were not well defined by discrete limits. As stimulus level was increased, loudness growth ceased before MAL was reached, i.e., no growth in loudness was observed above a given current level, and that level was below MAL. This occurred on some electrodes for subjects JWB and RFM. In such cases, MAL was taken to be the level where loudness growth saturated.

Absolute thresholds varied both among subjects and across electrodes within a subject. The lowest threshold of 36.1 dB *re*: 1 μA (64.2 μA) was seen on rEL06 from subject DVS, while the highest threshold of 53.4 dB (468.4 μA) was observed on rEL05 from subject RFM. Within a given subject, the largest threshold differences across electrodes were seen for subject DVS. This subject revealed unusually large threshold differences for adjacent electrodes rEL09, rEL10, rEL11, and rEL12, with the largest difference between rEL06 and rEL11 (9.6 dB). This curious pattern of alternating high and low absolute thresholds may reflect an internal problem with this subject's receiver/stimulator. Subject RFM also exhibited a large threshold difference between rEL05 and rEL15 (10 dB), but these electrodes were widely separated from one another.

Dynamic range, expressed as the difference between MAL and absolute threshold (in dB), also varied among subjects and across electrodes. Subject JWB exhibited the largest dynamic ranges across electrodes, averaging 10.8 dB and varying from 8.6 to 12.4 dB. Subject DVS exhibited the greatest variation in dynamic range across electrodes, between 5.5 and 13.5 dB, with an average dynamic range of 8.7 dB. Subjects EES and AMA had the smallest dynamic ranges, averaging 3.6 and 3.4 dB, respectively, and these were quite constant across electrodes. Such large differences in absolute threshold and dynamic range among subjects and across electrodes within the same subject provided a unique opportunity to examine relations between intensity discrimination and absolute threshold or dynamic range, which might stem from differences in surviving neural function.

B. Metrics for measuring intensity difference limens

Common metrics for specifying intensity discrimination in acoustic listeners are the intensity increment in dB $\{\Delta I_{\mathrm{dB}}=10\ \log(I+\Delta I)-10\ \log(I)\}$, the Weber fraction $\{Wf=\Delta I/I\}$, and the Weber fraction expressed in decibels $\{Wf_{\mathrm{dB}}=10\ \log(\Delta I/I)\}$, where I is the intensity of the acoustic stimulus in W/cm^2 (Viemeister, 1988). Of these, the Weber fraction in decibels yields the most constant variance in threshold estimates across stimulus level. Since a primary aim of the present study was to evaluate stimulus level effects on electrically elicited intensity discrimination, it was important to select a metric with this characteristic. Thus the Weber fraction in dB is used here. It will be shown later (Fig. 4) that this metric produces measures of intensity discrimination with constant variance across stimulus level, as in the acoustic case. Since the present stimuli are specified in terms of electric current, the Weber fraction may be specified as: $Wf=\Delta A^2/A^2+2\Delta A/A$, where A is current amplitude in μA (Pfingst *et al.*, 1983).

As noted previously, we refer to the curve describing Weber fractions in dB as a function of the stimulus level of the standard above absolute threshold, as a *Weber function*. Empirical Weber functions are well described by a power function of stimulus intensity relative to absolute threshold intensity as follows:

$$\Delta I/I=\beta(I/I_0)^{\alpha}, \tag{1a}$$

$$Wf_{\mathrm{dB}}=\alpha\cdot 10\ \log(I/I_0)+10\ \log(\beta), \tag{1b}$$

$$Wf_{\mathrm{dB}}=\alpha(\mathrm{dB\ SL})+\mathbf{b},\ \text{where}\ \ \mathbf{b}=10\ \log(\beta). \tag{1c}$$

Equation (1) has been used successfully to describe intensity discrimination as a function of sensation level in normal-hearing acoustic subjects (Jesteadt *et al.*, 1977; Schroder *et al.*, 1994). Equation (1a) expresses the Weber fraction ($\Delta I/I$) in terms of the ratio between the intensity of the standard (I) and the intensity at absolute threshold (I_0) for $I>I_0$, while Eqs. (1b) and (1c) express the Weber fraction in decibels (Wf_{dB}) in terms of the sensation level (SL) of the standard. The same equations can be used to specify intensity discrimination for electric simulation.

To illustrate the application of Eq. (1) to electric intensity discrimination, averaged Weber functions for two electrodes from subject TVB are shown in the left panel of Fig. 2. Both functions were fitted to Eq. (1c) by linear least-squares regression. The resulting parameters are given in Fig. 2 and the best fitting Weber functions are plotted as heavy shaded lines. An index of overall sensitivity to intensity change (β), given by the intercept (10 log $\beta=\mathbf{b}$) of Eq. (1c), was better for the bottom curve (−2.05 dB) than for the top curve (+1.66 dB). In addition, the exponent (α) of the Weber function, which defines the change in Weber fractions with intensity, is 2.5 times smaller (steeper negative slope) for the bottom curve (−1.96 dB/dB) than for the top curve (−0.78 dB/dB). This application of Eq. (1c), derived from a standard metric of intensity discrimination in normal acoustic hearing, demonstrates that differences in both the sensitivity term (β) and exponent (α) of the Weber function can be observed for electric stimulation on different electrodes.

Figure 2 also illustrates that dynamic range can influence measures of intensity discrimination. Dynamic range (DR) is specified as 20 log ($A_{\mathbf{M}}/A_0$), where $A_{\mathbf{M}}$ is the current at the maximum acceptable loudness level and A_0 is the current at absolute threshold.[3] In this example, the dynamic ranges for the two electrodes in the same subject are grossly different. Notice that the electrode with the smaller dynamic range (DR=5.6 dB) exhibits a Weber function with better sensitivity and a larger exponent than the electrode with the larger dynamic range (DR=12 dB). That is, both the slope and the intercept of the Weber function appear to vary inversely with dynamic range, which implies that normalizing the intensity dimension by the dynamic range should reduce the variability among slopes of Weber functions obtained

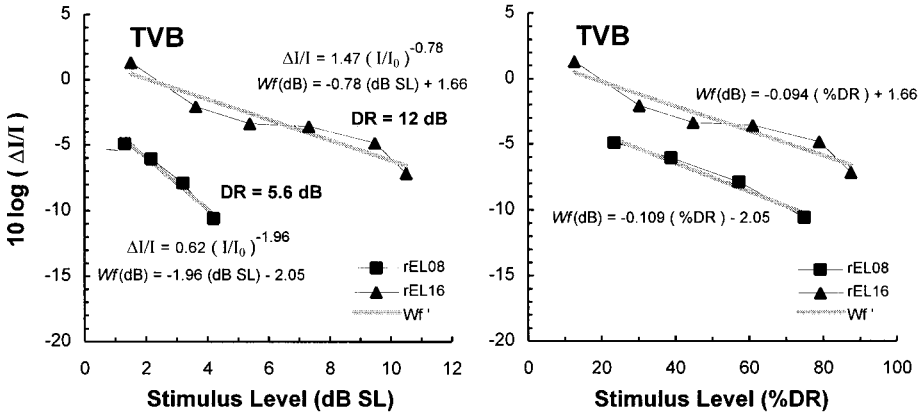

FIG. 2. Weber functions for two electrodes with different dynamic ranges from subject TVB. *Left panel*: Mean Weber fractions (in dB) plotted as a function of stimulus level in dB SL and fitted with Eq. (1). *Right panel*: Mean Weber fractions (in dB) plotted as a function of stimulus level expressed as a percentage of the dynamic range (DR) for each electrode and fitted with Eq. (2). Parameters from least-squares fits to the two equations are given in the panels. Normalization of stimulus level by DR, shown in the right panel, tends to equalize slopes of Weber functions.

from electrodes with disparate dynamic ranges. This is accomplished by modifying the exponent in Eq. (1) as follows:

$$\Delta I/I = \beta (I/I_0)^{\alpha(\mathrm{DR}/100)}. \tag{2a}$$

This is equivalent to specifying the Weber fraction (in dB) in terms of stimulus level expressed as a percentage of dynamic range (%DR):

$$Wf_{\mathrm{dB}} = \mathbf{a}\left\{ \frac{20\log(A/A_0)}{20\log(A_M/A_0)} \right\} * 100 + \mathbf{b}, \tag{2b}$$

$$Wf_{\mathrm{dB}} = \mathbf{a}\left\{ \frac{\mathrm{SL(dB)}}{\mathrm{DR(dB)}} \right\} * 100 + \mathbf{b}, \tag{2c}$$

$$Wf_{\mathrm{dB}} = \mathbf{a}\{\%\mathrm{DR}\} + \mathbf{b}, \quad \text{where} \quad \mathbf{b} = 10\log(\beta). \tag{2d}$$

Thus the slope terms in Eq. (1c) and Eq. (2d) are related by the DR according to the equation:

$$\alpha = \mathbf{a} \cdot (100/\mathrm{DR}). \tag{3}$$

The right-hand panel of Fig. 2 demonstrates the results of normalizing the stimulus level dimension by the dynamic range as in Eq. (2d). Visual inspection of Fig. 2 suggests that Eq. (1) and Eq. (2) provide good quantitative representations of Weber fractions as a function of stimulus level (r^2 values are 0.97 and 0.91 for the lower and upper curves, respectively). With the normalization to DR, slopes of the Weber functions for TVB's two electrodes are nearly equal, at about -0.10 dB/%DR (-0.094 and -0.109), and the primary distinction between the two functions is a difference in sensitivity ($+1.66$ vs -2.05). This suggests that the Weber fraction for electric stimulation is a function of the level of the standard expressed in %DR, a premise that will be evaluated below. However, we will first consider the variance associated with adaptively determined Weber fractions and some limitations inherent to Weber fraction measurements.

C. Variability of Weber fractions

The variability that can be expected with electric Weber fractions is illustrated in Fig. 3, which shows Weber fractions obtained during multiple test sessions from representative electrodes in all eight subjects. Each panel shows Weber fractions (Wf_{dB}) obtained from a single electrode, plotted as a function of stimulus level in %DR. The top two rows of panels show data from the four subjects for whom six electrodes were tested; the bottom row shows data from the four subjects for whom three electrodes were tested. Individual Weber fraction estimates are shown by shaded diamonds and the means of those estimates are connected by dark lines. Other features of Fig. 3 will be discussed later. Test–retest variability was sometimes quite large (e.g., JWB rEL14, at the highest two stimulus levels). However, there was no systematic change in variability with stimulus level, even though many of the average Weber fractions improved with increasing level.

Standard deviations for multiple Weber fraction estimates are shown in Fig. 4 for all of the electrodes tested in five subjects (JWB, TVB, DVS, JPB, EES) whose sensitivity was not strongly limited by the resolution limits of their receiver/stimulators (see below). The left panel shows standard deviations for Weber fractions (in dB) as a function of stimulus level in %DR. Regression analysis revealed that the variance did not change significantly with stimulus level ($p = 0.54$). The predicted average standard deviation across tests increased from 1.26 dB at 5% of DR to 1.36 dB at 95% of DR, a change of less than 7%. Standard deviations for another common index of intensity discrimination, the just detectable intensity increment in dB (ΔI_{dB}), are shown in the right-hand panel of Fig. 4. For the ΔI_{dB} index, the variance did change significantly with stimulus level ($p = 0.0001$). Average standard deviations across tests decreased from 0.35 dB at 5% of DR to 0.17 dB at 95% of DR, a change of more than 100%. This result is similar to that reported for normal acoustic listeners (Viemeister, 1988) and supports the use of the Weber fraction (in dB) as a measure of intensity discrimination for electric stimulation.

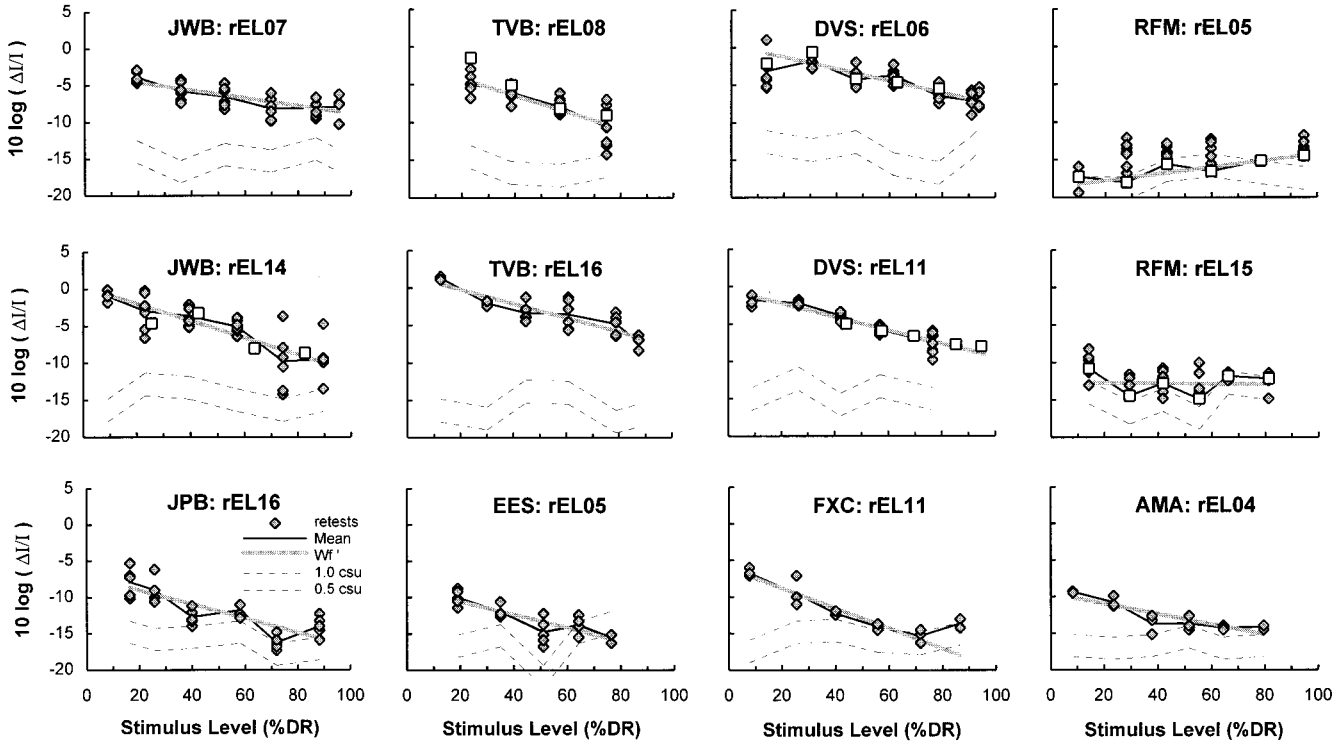

FIG. 3. Representative Weber fractions obtained from multiple tests with a 3AFC adaptive procedure. Individual estimates from the adaptive procedure are shown (shaded diamonds), along with mean Weber fractions at each stimulus level (connected by dark solid lines) and the Weber function (Wf') fitted to those means using Eq. (2) (wide shaded line). Corresponding Weber fractions obtained from psychometric functions for intensity discrimination are shown for some subjects (open squares). The intensity resolution limits of the implanted receiver/stimulator, corresponding to 1.0 and 0.5 CSUs, are shown at the bottom of each panel (thin dashed lines). The adaptive Weber fractions around 80% DR for RFM were all better than 0.5 CSUs and are not plotted.

D. Intensity resolution limits of implanted receiver/stimulators

In Fig. 3, the mean Weber fractions at different stimulus levels are connected by dark lines, and the Weber functions resulting from a linear least-squares fit of those means to Eq. (2d) are shown by the wide shaded lines. Preliminary examination of these mean data suggests that Weber fractions tend to improve with stimulus level when large Weber fractions exist, and they tend to remain constant with stimulus level when highly sensitive Weber fractions exist. The trend toward improved Weber fractions with stimulus level was evident throughout the entire dynamic range in subjects JWB,

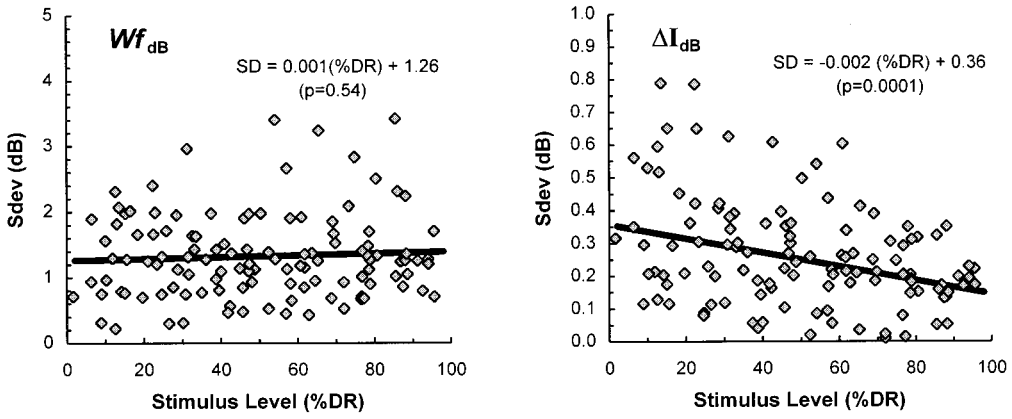

FIG. 4. Scattergrams showing standard deviations for multiple DL estimates on individual electrodes, plotted as a function of stimulus level expressed in percent dynamic range (%DR). *Left-hand panel*: Standard deviations for DLs expressed as Weber fractions in decibels as a function of the stimulus level (%DR). The best-fit linear regression is shown by the wide dark line. The coefficient of determination for the regression (r^2) was zero, indicating no statistically significant relationship between S_{dev} and %DR ($p=0.54$). *Right-hand panel*: Standard deviation for DLs expressed as intensity increments (ΔI_{dB}) in decibels. The best-fit linear regression is shown by the heavy line. The regression coefficient was significant ($p=0.0001$). The regression equation and the derived parameters are also shown in each panel.

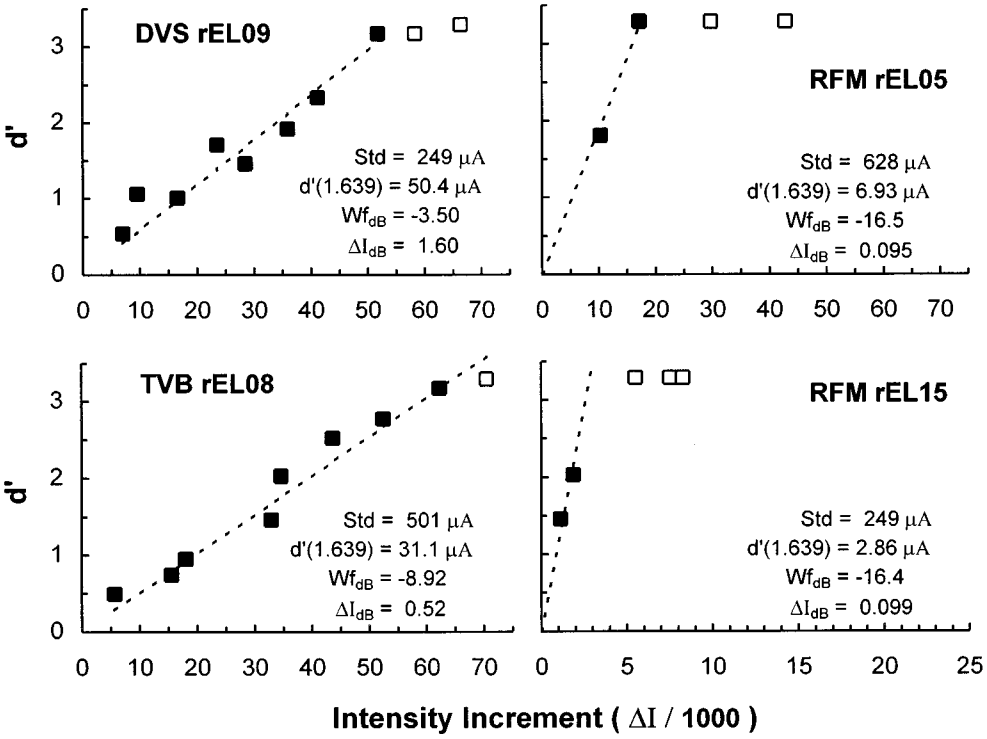

FIG. 5. Representative psychometric functions for intensity discrimination. Intensity discrimination performance in d' units is plotted against stimulus intensity increment size, ΔI, expressed in intensity units ($\Delta I = 2A*\Delta A + \Delta A^2$). Psychometric functions were fitted with straight lines through zero using least-squares regressions (dashed lines) on data points shown by filled squares (data points shown by unfilled squares were not used in the regressions). Each panel is for a different electrode. Two psychometric functions for subjects with poorer sensitivity to intensity change are shown in the left-hand panels. Two psychometric functions for different electrodes from the subject with the best sensitivity to intensity change are shown in the right-hand panels. Note, from the tic spacing, that the range on the abscissa for the bottom right hand panel is less than half that for the other panels. The level of the standard (Std) in μA and the stimulus increment in μA that corresponds to a d' of 1.63 are listed in each panel, along with the corresponding Weber fraction (Wf_{dB}) and intensity increment in decibels (ΔI_{dB}). For subjects RFM and TVB, the consecutive symbols correspond to the smallest current steps achievable with their implanted receiver/stimulators. For subject DVS, consecutive symbols correspond to twice the smallest current step.

TVB, and DVS. Their Weber fractions were among the largest measured. Improvement in the Weber fraction with stimulus level was evident only over the bottom half or two thirds of the dynamic range in subjects JPB, EES, FXC, and AMA. In the upper half or one third of their dynamic ranges, where Weber fractions were most sensitive, Weber fractions were relatively constant. Finally, relatively constant Weber fractions were seen across the entire dynamic range in subject RFM. His Weber fractions were among the most sensitive measured.

This trend toward constant Weber fractions in regions of highly sensitive intensity discrimination can be partly explained by examining the smallest CSUs realizable with each individual's implanted receiver/stimulator. Weber fractions corresponding to comparison stimuli that were 1 CSU above the standard and $\frac{1}{2}$ CSU above the standard, respectively, are indicated in each panel of Fig. 3 by the upper and lower thin dashed lines. Notice that Weber fractions from subjects with relatively flat Weber functions (RFM), or regions of relatively constant Weber fractions in the upper half of the dynamic range (JPB, EES, FXC, and AMA), also exhibited Weber fractions that were closest to the limits imposed by a 1-CSU step. In these subjects with extremely small Weber fractions, it appears that the resolution limit of 1 CSU precluded measurement of better Weber fractions, especially at the highest stimulus levels tested.

E. Psychometric functions for intensity discrimination

The observation of extremely small Weber fractions in one of the earlier subjects tested (RFM) prompted the measurement of psychometric functions as a means of validating the adaptive Weber fractions. Psychometric functions were subsequently obtained for 21 of 24 electrodes tested with adaptive Weber fractions in four subjects (DVS, JWB, RFM, and TVB). Four representative psychometric functions are shown in Fig. 5. Intensity discrimination performance is specified by d' as a function of the increment in intensity (ΔI) between the standard and the comparison stimulus. Linear regression with a zero intercept permitted estimation of the ΔI corresponding to a d' of 1.63, which is the performance level tracked by the 3AFC adaptive procedure (Hacker and Ratcliff, 1979). The corresponding Weber fraction in dB is listed in each panel, along with the corresponding ΔI_{dB} value, the increment in μA, and the level of the standard in μA. Psychometric functions in the left-hand panels are from two subjects, DVS and TVB, who exhibited poorer than average sensitivity to intensity increments. For

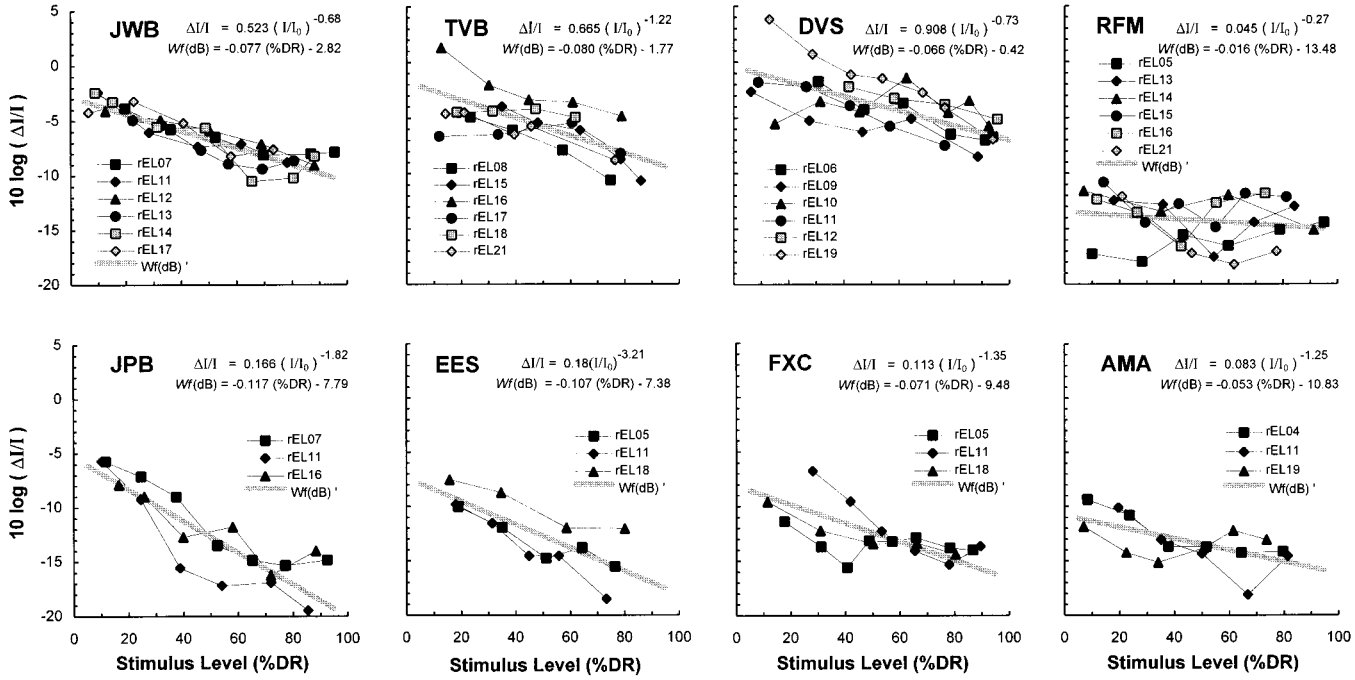

FIG. 6. Weber functions from individual electrodes in eight subjects. Mean Weber fractions (in dB) are plotted as a function of stimulus level expressed as percent of dynamic range (%DR). Each panel contains Weber functions obtained on different electrodes from a single subject. Different electrodes are coded by different symbols within each panel. Each of the Weber functions from individual electrodes was fitted to Eq. (2) and the average slope and intercept was used to generate a composite Weber function for each subject, shown by the wide shaded curve in each panel. The average fitting parameters are shown within each panel for Eq. (1) in terms of dB SL and for Eq. (2) in terms of %DR.

these subjects, the rising portion of the psychometric function is well defined by a linear function (dashed lines) with a relatively flat slope. The Weber fractions estimated from these psychometric functions (−3.50 and −8.92 dB) are within the range of those obtained with the adaptive procedure. The two psychometric functions in the right-hand panels are from the subject who exhibited the smallest Weber fractions (RFM). Consecutive symbols represent the smallest CSUs available from this subject's receiver/stimulator. For rEL05, performance better than $d'=1.63$ was exhibited at 1 CSU, the intensity resolution limit of the receiver/stimulator. The fitted psychometric functions have extremely steep slopes, yet the corresponding Weber fractions (−16.5 and −16.4 dB) are within the range of those obtained with the adaptive procedure.

For some of the electrodes shown in Fig. 3, Weber fractions estimated from psychometric functions are shown as unfilled squares in Fig. 3. For example, the psychometric functions from RFM shown in Fig. 5 correspond to data points in Fig. 3 (unfilled squares) at stimulus levels of 29 and 55%DR on electrodes rEL 05 and rEL 15, respectively. Examination of adaptive thresholds at these stimulus levels (Fig. 3) indicates that the Weber fractions estimated from psychometric function slopes correspond to the lowest Weber fractions estimated by the adaptive procedure.[4] In the other subjects, examination of adaptive Weber fractions and those calculated from psychometric functions, some of which are plotted in Fig. 3, indicated acceptable correspondence between the two types of estimates. This led us to conclude that the adaptive procedure provided a valid index of intensity discrimination. A secondary but critical finding was that psychometric functions were monotonic and d' was linear with ΔI. Psychometric functions must be monotonic for valid adaptive measures to be obtained.

F. Weber fractions as a function of stimulus intensity

Figure 6 shows the mean Weber fractions (in dB) as a function of stimulus level (in %DR) for all of the electrodes tested in each of the eight subjects. Preliminary examination of these data indicated that Weber fractions tended to improve with stimulus level. Furthermore, the improvement with level seemed to be the greatest on those electrodes where Weber fractions were poorest at low levels (e.g., JWB), and to be the least where Weber fractions were the best at low levels (e.g., RFM). To examine these observations further, linear regressions were performed on the mean Weber fractions as a function of stimulus level. Table III summarizes the results of the regression analyses for individual electrodes. (Regression lines for individual electrodes are not plotted in Fig. 6; wide shaded lines represent composite Weber functions for each subject, discussed below.)

Four parameters are given in Table III for each regression. Mean Weber fractions were fitted to Eq. (2c) with a least-squares procedure to yield an estimate of the slope (**a**) and the intercept (**b**) of the Weber function in terms of %DR. The coefficient of determination ($\mathbf{r}^2$) provided a measure of the relative variance accounted for by the regression. F ratios were calculated to determine if the slopes were significantly different from a slope of zero. Finally, the exponent (α) in

TABLE III. Parameters from regression analyses of Weber functions, specified in terms of dB SL[$Wf=\beta(I/I_0)^{\alpha}$], and specified in terms of percent dynamic range[$Wf=\beta(I/I_0)^{\alpha(\mathrm{DR}/100)}$]; $\mathbf{a}=\alpha(\mathrm{DR}/100)$.

		JWB					TVB		
rEL	10 log(β)	α	**a**	$\mathbf{r^2}$	rEL	10 log(β)	α	**a**	$\mathbf{r^2}$
07	−3.50	−0.45	−0.05	0.8609[b]	08	−2.05	−1.95	−0.11	0.9766[b]
11	−2.65	−0.69	−0.08	0.8480[a]	15	0.69	−1.86	−0.12	0.9326[b]
12	−2.92	−0.61	−0.06	0.9667[b]	16	1.66	−0.78	−0.09	0.9104[b]
13	−3.47	−0.91	−0.08	0.8168[b]	17	−4.84	−0.67	−0.03	0.2687
14	−1.52	−0.91	−0.11	0.8802[b]	18	−2.77	−0.83	−0.05	0.6004
17	−2.85	−0.57	−0.07	0.7593[a]	21	−3.32	−1.63	−0.07	0.9227[b]
		DVS					RFM		
rEL	10 log(β)	α	**a**	$\mathbf{r^2}$	rEL	10 log(β)	α	**a**	$\mathbf{r^2}$
06	0.32	−0.63	−0.08	0.9051[b]	05	−18.65	0.75	0.04	0.7418
09	−2.81	−1.17	−0.06	0.7825[a]	13	−13.01	−0.32	−0.02	0.0618
10	−4.26	0.02	0.00	0.0034	14	−11.38	−0.47	−0.03	0.5778
11	−0.45	−1.47	−0.09	0.9628[b]	15	−12.62	−0.06	0.00	0.0043
12	−0.07	−0.47	−0.05	0.9766[b]	16	−13.92	0.20	0.01	0.0238
19	4.77	−1.64	−0.12	0.9683[b]	21	−11.29	−3.24	−0.09	0.6772
		JPB					EES		
rEL	10 log(β)	α	**a**	$\mathbf{r^2}$	rEL	10 log(β)	α	**a**	$\mathbf{r^2}$
07	−10.51	−1.30	−0.08	0.7192	05	−8.75	−2.92	−0.09	0.8631[a]
11	−5.81	−2.56	−0.17	0.8560[b]	11	−7.00	−4.09	−0.15	0.9633[b]
16	−7.07	−1.53	−0.10	0.7443[a]	18	−6.38	−2.46	−0.08	0.9056[a]
		FXC					AMA		
rEL	10 log(β)	α	**a**	$\mathbf{r^2}$	rEL	10 log(β)	α	**a**	$\mathbf{r^2}$
05	−12.76	−0.27	−0.01	0.1019	04	−9.56	−1.309	−0.07	0.8012[b]
11	−6.11	−2.04	−0.14	0.9771[b]	11	−9.45	−2.66	−0.09	0.5976
18	−9.58	−1.51	−0.06	0.8783[b]	19	−13.47	0.04	0.00	0.0012

[a]$p\leq 0.05$.
[b]$p\leq 0.01$.

Eq. (1), which defines the slope of the Weber function in terms of dB SL, was calculated from **a** using Eq. (3) and the corresponding DR on each electrode. Table III indicates that the Weber function slopes were clearly negative for 23 of 30 electrodes tested in seven subjects (JWB, TVB, DVS, JPB, EXC, EES, and AMA). Slopes for five of the other seven electrodes in these subjects, although negative, were not significantly different from zero.

Examination of the mean Weber functions in Fig. 6 indicates that, for individual subjects, slopes tended to be similar across electrodes. There were small differences among electrodes but no obvious trends toward dramatically different Weber functions from electrodes in the apical versus the basal region of the electrode array. These observations were confirmed by statistically insignificant regressions ($p>0.40$) between slopes (**a**) or intercepts (**b**) and electrode number (see Table IV). Therefore, a composite Weber function was calculated for each subject from the average slope and average intercept across electrodes. These composite Weber functions are shown by the wide shaded lines in Fig. 6. The average slopes and intercepts for each subject are listed in each panel, in the form of parameters for Eqs. (1) and (2). The composite Weber function intercepts varied from −0.42 dB ($\Delta I_{\mathrm{dB}}=2.8$) in subject DVS to −13.48 dB ($\Delta I_{\mathrm{dB}}=0.19$) in subject RFM. Expressed in terms of %DR [Eq. (2)], the composite Weber function slopes varied from −0.12 (JPB) to −0.02 dB/%DR (RFM). Finally, expressed in terms of dB SL [Eq. (1)], the composite Weber function slopes varied from −3.21 (EES) to −0.27 dB/dB (RFM). Among the seven subjects whose Weber fractions were not markedly restricted by the intensity resolution limits of their receiver/stimulators, the average composite Weber function slope was −0.08 dB/%DR. This corresponds to an 8-dB improvement in the Weber fraction over the entire dynamic range. In terms of dB SL, the average Weber function exponent in the same subjects was −1.5 [Eq. (1a)].

Examination of the mean Weber function for rEL 10 from subject DVS, shown as triangles in Fig. 6, reveals that Weber fractions increased with level up to about 60% of the dynamic range, and then decreased with further increases in stimulus level. This electrode also exhibited an unusually sensitive absolute threshold (see Fig. 1), which was accompanied by much higher absolute thresholds on neighboring electrodes (rEL09 and rEL11). The reason for the large differences in absolute threshold on adjacent electrodes is unclear, but it is worthy of note that an atypical Weber function was associated with the more sensitive absolute threshold. Perhaps the more sensitive threshold is spurious because of local characteristics of the implanted array.

One subject (RFM) exhibited relatively flat Weber functions on all electrodes, none of which had slopes significantly different from zero. From Fig. 6, it can be seen that this subject demonstrated the smallest Weber fractions. Also notice that the Weber functions from AMA showed shallow

TABLE IV. Correlations among Weber-function parameters (**a**,**b**,α), dynamic range (DR), absolute threshold (THS), electrode number (EL#), and pitch-ranking parameters: cumulative d' at 0.75-mm spatial separation (Cum d') and spatial separation for $d'=2.0$ [SS($d'=2$)].

	b	(p)	α	(p)	DR	(p)	THS	(p)	EL#	(p)
a	**−0.55**	<0.001	**+0.80**	<0.001	0.02	0.917	−0.14	0.401	−0.04	0.805
b			−0.17	0.322	**0.50**	0.002	**−0.48**	0.003	+0.14	0.400
α					**0.49**	0.002	**−0.37**	0.025	−0.08	0.630
DR							**−0.67**	<0.001	−0.14	0.416
THS									−0.02	0.925

	Cum d'	(p)	SS ($d'=2$)	(p)	DR	(p)	THS	(p)
b	**−0.84**	0.009	**+0.74**	0.036				
α	+0.32	0.438	−0.18	0.666				
Wf_{dB} (25%DR)	**−0.78**	0.022	**+0.72**	0.044	**0.57**	<0.001	**−0.58**	<0.001
Wf_{dB} (50%DR)	−0.69	0.057	+0.68	0.065	**0.61**	<0.001	**−0.65**	<0.001
Wf_{dB} (75%DR)	−0.58	0.133	+0.61	0.108	**0.61**	<0.001	**−0.69**	<0.001

negative slopes in the lower half of the dynamic range but relatively flat slopes in the upper half where Weber fractions were extremely sensitive. This tendency, toward relatively constant Weber fractions where sensitivity was best, was also exhibited for some electrodes in three of the subjects who had significantly negative Weber-function slopes (JPB, EES, and FXC). In support of this observation, comparisons of slopes and intercepts among all electrodes tested revealed a moderate but significant negative correlation of −0.55 between slopes (**a**) and intercepts (**b**) across subjects (see Table IV). A contributing factor to this tendency toward constant Weber fractions where sensitivity was best may be the resolution limits of the implanted receiver/stimulators. Examination of data for electrodes with constant Weber fractions over part or all of the dynamic range revealed that the Weber fractions were usually near to or below the 1-CSU limit. It is, therefore, likely that the slopes of these Weber functions were limited by the resolution limits of the implanted receiver/stimulator. Had smaller current steps been available, steeper negative slopes might have been observed.

To summarize, regression analyses of Weber functions indicated that Weber fractions generally improved with stimulus level across the dynamic range. Improvement in Weber fractions with stimulus level averaged 8 dB over the dynamic range, and the improvement appeared to be inversely related to the overall sensitivity of the Weber function, possibly because the smaller Weber fractions at high stimulus levels were limited by the intensity resolution limits of the implanted receiver/stimulators. There were no consistent differences between Weber functions obtained from electrodes in different regions of the implanted array.

G. Correlations with absolute threshold and dynamic range

Recall, from Fig. 1, that absolute threshold and dynamic range varied considerably among subjects and even across electrodes in the same subject (e.g., DVS and RFM). Such differences afforded the opportunity to examine the relation between Weber fractions, absolute threshold and dynamic range. Since Weber fractions are level dependent, Weber fractions were calculated at 25%, 50%, and 75%DR from the fitted Weber functions for individual electrodes using the parameters in Table III and Eq. (2). These values, along with the Weber-function fitting parameters, were then compared with measures of absolute threshold and dynamic range by linear regression analysis.

Correlation coefficients describing relations among the Weber-function parameters, dynamic range, absolute threshold and electrode number are shown in Table IV. Exponents of the Weber power function (α) were positively correlated with dynamic range (DR) and negatively correlated with absolute threshold (THS), although neither correlation was exceptionally strong. After normalizing to dynamic range, slopes (**a**) were no longer correlated with either dynamic range or absolute threshold. Sensitivity constants (**b**) were positively correlated with DR and were negatively correlated with THS and Weber-function slope (**a**). Electrode number was not correlated with any of the other variables.

Table IV also shows that Weber fractions were inversely proportional to absolute threshold, especially in the upper half of the dynamic range (e.g., at 75% DR, $r=-0.69$, $p<0.001$). To illustrate this relation, a scattergram of Weber fractions at 75%DR vs. absolute threshold is shown in the left-hand panel of Fig. 7. Examination of within- and across-subject data in this figure reveals that there was a strong tendency for subjects with higher absolute thresholds to exhibit better Weber fractions, but there was not a tendency, within subjects, for electrodes with higher absolute thresholds to exhibit better Weber fractions. The relation between size of the Weber fraction and absolute threshold across electrodes was significant ($p<0.05$) for only two subjects (TVB and RFM) at each of two stimulus levels (50% and 75% of DR).

Calculated Weber fractions at all three stimulus levels were also significantly related to dynamic range (Table IV). This was expected due to a clear inverse relation between absolute threshold and dynamic range across subjects ($r=-0.67$, $p<0.001$), which is illustrated in the right-hand panel of Fig. 7. Again, the relation was not apparent across electrodes within individual subjects; only DVS exhibited a significant correlation ($p<0.05$) between dynamic range and absolute threshold across electrodes.

H. Weber fractions and electrode pitch ranking

Seven of the subjects in this study had previously participated in an investigation of electrode ''pitch'' ranking

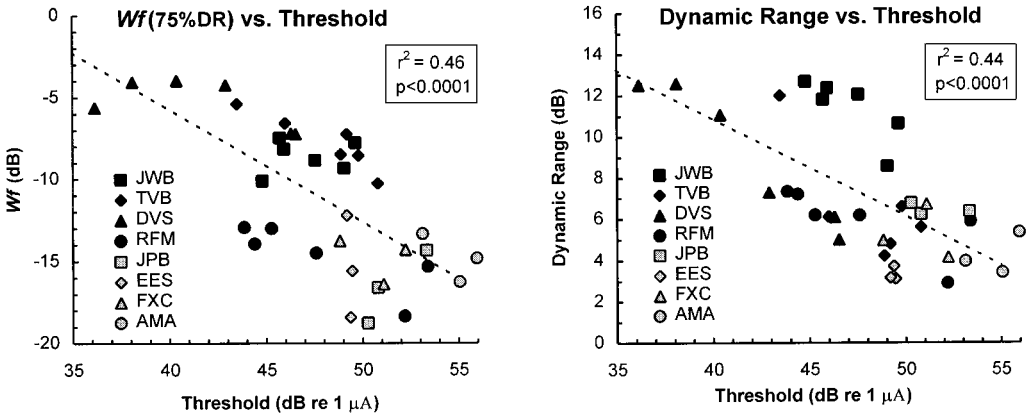

FIG. 7. Scattergrams showing the relationship between Weber fractions, dynamic range and absolute threshold. *Left-hand panel*: Weber fractions in dB calculated at 75% of dynamic range are plotted against absolute threshold. *Right-hand panel*: Dynamic range (in dB) is plotted against absolute threshold. Data from multiple electrodes are shown with identical symbols; different symbols are for individual subjects. Results of the linear regression across subjects and electrodes are given in the insert within each panel.

(Nelson *et al.*, 1995). The eighth subject (FXC) was also tested on this task following the intensity-DL measurements. The ability of subjects to discriminate ''pitch'' differences on the basis of electrode location presumably requires the existence of a relatively large and tonotopically organized population of surviving neurons. Therefore, comparisons between pitch ranking performance and intensity discrimination performance may help to elucidate the physiological mechanisms underlying both abilities.

Pitch-ranking stimuli were 500-ms bursts of 200-μs phase biphasic pulses presented at a rate of 125 Hz and at a comfortable loudness level. Pairs of stimuli were presented on electrodes separated by a variable distance and subjects were asked to judge which of the two stimuli sounded higher in pitch or ''sharper'' (2AFC). A wide range of pitch-ranking abilities was seen across subjects. Some subjects could consistently distinguish stimuli presented on adjacent electrodes, whereas others could not discriminate the pitch of adjacent electrodes at all and required large spatial separations (SSs) between electrodes before they could tell that a stimulus presented on one electrode was higher in pitch than one presented on a comparison electrode. For purposes of comparing pitch ranking and intensity discrimination abilities, pitch-ranking scores were specified in terms of the cumulative d' score achieved across all adjacent electrodes (cumulative d' for SS=0.75 mm) and in terms of the spatial separation required to achieve a d' score of 2.0 (SS for $d'=2$).

Correlations between pitch-ranking indices and Weber-function parameters are shown in Table IV. Composite Weber-function parameters and Weber fractions calculated from those parameters at 25%, 50%, and 75% of dynamic range were compared with cumulative d' scores and spatial separation scores using linear regression procedures. Pitch ranking scores and intensity discrimination scores were clearly related: Cumulative d' scores were negatively correlated with Weber-function sensitivity (10 log β=**b**) and the calculated Weber fraction at 25% of dynamic range. In addition, the spatial separation required to reach a d' of 2.0 was positively correlated with the same two intensity discrimination parameters. Correlations between pitch-ranking measures and calculated Weber fractions at 50% and 75% DR also approached (but failed to reach) significant values; the restricted range of Weber fractions at these higher stimulus levels probably limited the magnitude of correlations. These results indicate that subjects who can best discriminate pitch differences on closely spaced electrodes also exhibit the smallest Weber fractions.

I. Amplitude DLs as a constant proportion of dynamic range

Shannon (1983) characterized amplitude discrimination from one cochlear implant subject (CB) as being a constant 4%–8% of the dynamic range. This observation led us to consider the possibility that DLs correspond to a constant proportion of the dynamic range of electric stimulation. Since Shannon was assessing amplitude DLs, the hypothesis suggested by his observation is that $\Delta A/\mathrm{DR}_A$ is constant, both across the dynamic range of any particular electrode, and across electrodes with differing dynamic ranges. Here, ΔA is the just detectable increment in μA, or amplitude DL, and DR_A is the dynamic range expressed in μA ($\mu\mathrm{A}_{\mathrm{MAL}}-\mu\mathrm{A}_{\mathrm{THS}}$).

To examine this hypothesis, Weber fractions obtained from 36 electrodes in eight subjects were transformed into amplitude DLs: $\Delta A/\mathrm{DR}_A\cdot 100$ or $\Delta A(\%\mathrm{DR}_A)$. The transformed data are shown in Fig. 8, where mean amplitude DLs for individual electrodes are plotted as a function of stimulus level in %DR. Notice that the ordinate has been expanded for three subjects (TVB, DVS, and EES) to accommodate their larger amplitude DLs. Linear regression analyses were used to determine whether mean amplitude DLs improved with %DR. In addition, a composite amplitude DL curve was constructed for each subject by averaging the resulting regression coefficients across electrodes. These composite curves are shown in Fig. 8 (heavy shaded lines), along with the fitting equations that describe them.

For six subjects (TVB, DVS, JPB, EES, FXC, and

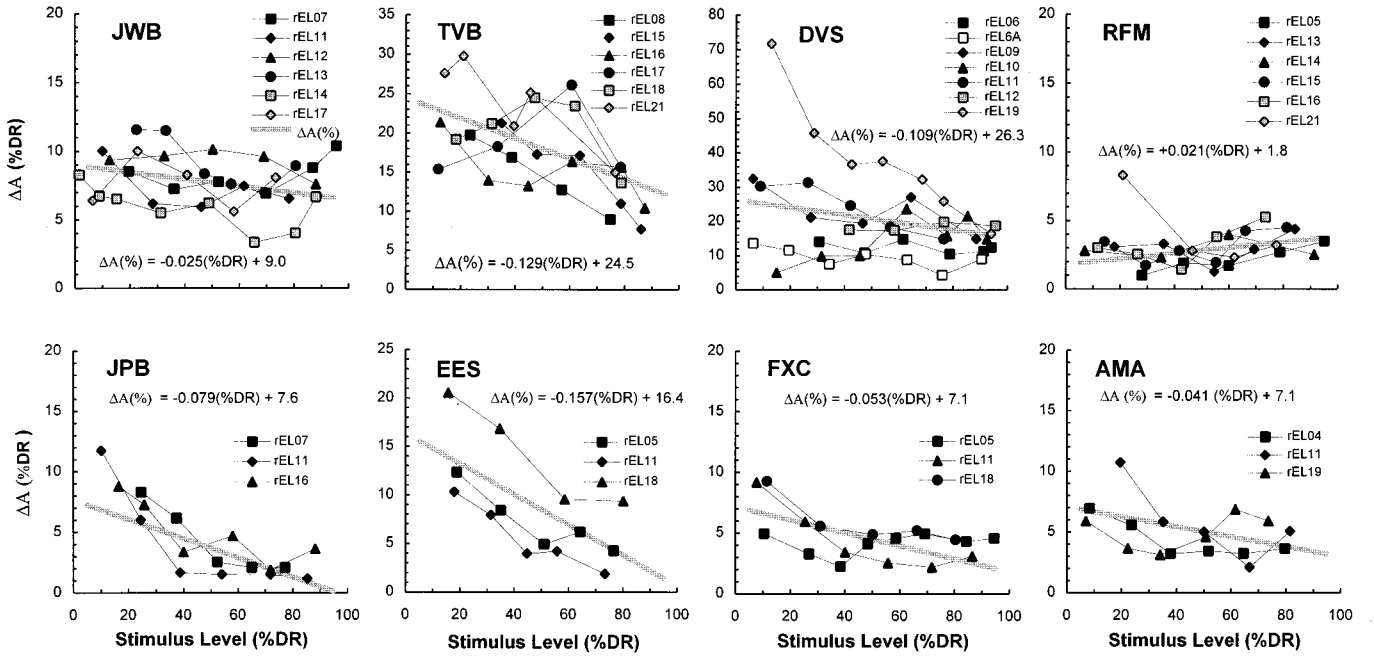

FIG. 8. Amplitude DLs from individual electrodes in eight subjects, expressed as a percentage of dynamic range (in μA). Mean amplitude DLs, expressed as percent of dynamic range (ΔA in %DR), are plotted as a function stimulus level and are referred to as amplitude DL curves. Each panel contains the mean amplitude DL curves obtained from different electrodes in a single subject. Different electrodes are coded by different symbols within each panel. Each amplitude DL curve was fitted by linear least-squares regression, and the average slope and intercept across electrodes was used to generate a composite amplitude DL curve for each subject, which is shown by the wide shaded curve in each panel. The average fitting parameters are also given within each panel. Note that the ordinate is modified for TVB, DVS, and EES to accommodate larger DLs.

AMA), amplitude DLs were not a constant proportion of the dynamic range, either across electrodes or across stimulus levels. Results of linear regression analyses for individual electrodes indicated that data from nearly half of the electrodes (11 out of 24) were well fit ($p<0.01$) by linear functions with negative slopes. Figure 8 shows that amplitude DLs tended to improve with stimulus level in these six subjects, although this was not the case for all electrodes in every subject. For example, for subject DVS, some electrodes exhibited negative slopes while others exhibited flat or even positive slopes. In four subjects (JPB, EES, FXC, and AMA), amplitude DLs improved substantially with stimulus level in the lower half of the dynamic range, but remained relatively constant in the upper half of the dynamic range (see bottom row of panels in Fig. 8). In each case but one (EES, rEL18), amplitude DLs in the upper half of the dynamic range were artificially restricted by the intensity resolution limits of the implanted receiver/stimulator, and this prevented us from estimating ''true'' DLs. In three subjects (TVB, DVS, and EES) intercepts of the amplitude DL curves for different electrodes varied considerably, indicating that amplitude DLs were also variable across electrodes. For example, intercepts for subject DVS decreased from 58% of DR on rEL19 to 4% of DR on rEL10.[5] Thus amplitude DLs or six of eight subjects were not constant across stimulus level for a majority of the electrodes tested.

In two subjects (JWB and RFM), curves for individual electrodes tended to cluster together and their slopes were relatively flat or positive, suggesting that a constant amplitude DL across levels and electrodes might describe their data. Closer inspection showed that DLs for one of these subjects (RFM) approached the resolution limits of the implanted receiver/stimulator throughout the entire dynamic range and that ''true'' DLs may not have been measured. Thus only subject JWB yielded amplitude DLs that corresponded to a relatively constant percentage (7%–13%) of dynamic range.[6]

In summary, our data suggest that amplitude DLs are not constant across dynamic range and that the appearance of constant DLs may reflect the resolution limits of implanted receiver/stimulators.

J. Number of steps for coding intensity

Envelope cues have been shown to be particularly important for transmitting speech information through cochlear prostheses (Van Tasell *et al.*, 1992). Critical to that process is the accurate representation of intensity changes over time. The number of resolvable intensity steps available to represent envelope cues should directly affect the amount of envelope information transmitted, with a larger number of resolvable intensity steps leading to better resolution of envelope detail. The fact that Weber fractions improve substantially with intensity, precludes an estimate of the number of discriminable intensity steps from a single measurement. However, such estimates can be calculated from the composite Weber functions obtained here. This was done for each subject in the present study by simply cumulating consecutive discriminable intensity steps from the composite Weber functions shown in Fig. 6. Representative results of those

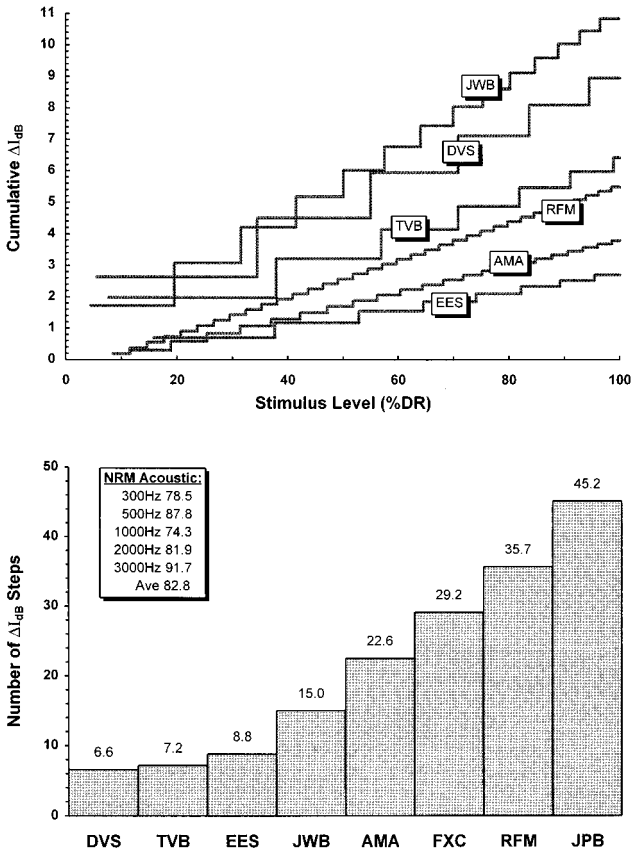

FIG. 9. Cumulative discriminable intensity steps across dynamic range and the number of discriminable intensity steps per subject. *Upper panel*: Cumulative ΔI_{dB} $\{10\log(I+\Delta I)-10\log(I)\}$ as a function of stimulus level in percent dynamic range (%DR in dB), which were calculated from the composite Weber functions in Fig. 6. Curves for JPB and FXC were not plotted because they overlapped with the curve for RFM. *Lower panel*: The total number of discriminable intensity steps across dynamic range is given for each of the eight subjects. The total number of discriminable intensity steps for normal acoustic hearing, calculated from Weber fractions reported by Schroder *et al.* (1994), are shown for each of five frequencies within the inset.

TABLE V. Fitting parameters for Weber functions obtained with electric stimulation and acoustic stimulation in terms of dB SL $[Wf=\beta(I/I_0)^{\alpha}]$ and in terms of %DR $[Wf=\beta(I/I_0)^{\alpha(\mathrm{DR}/100)}]$; $\mathbf{a}=\alpha(\mathrm{DR}/100)$.

	Electric stimulation		
Present study:	10 log (β)	α	**a**
DVS	−0.42	−0.73	−0.07
TVB	−1.77	−1.22	−0.08
JWB	−2.82	−0.68	−0.08
EES	−7.38	−3.21	−0.11
JPB	−7.79	−1.82	−0.12
FXC	−9.48	−1.35	−0.07
AMA	−10.83	−1.25	−0.05
RFM	−13.48	−0.27	−0.02
Shannon (1983):	10 log (β)	α	**a**
EL01,02	−2.67	−0.52	−0.13
EL05,06	−4.55	−0.38	−0.07
EL15,16	−2.61	−0.69	−0.15
Dillier *et al.* (1983):	10 log (β)	α	**a**
RG	−10.27	−0.87	−0.10
EP	−20.40	−0.07	−0.01
Pfingst and Rai (1990):	10 log (β)	α	**a**
M1	1.37	−0.49	−0.10
M2	1.39	−0.33	−0.08
M3	2.00	−0.49	−0.12
M4	2.18	−0.69	−0.11
	Acoustic stimulation		
Jesteadt (1977):	10 log (β)	α	**a**
	−3.34	−0.07	−0.06
Schroder *et al.* (1994):	10 log(β)	α	**a**
300 Hz	−1.68	−0.09	−0.07
500 Hz	−2.30	−0.07	−0.06
1000 Hz	−0.30	−0.08	−0.08
2000 Hz	0.60	−0.11	−0.10
3000 Hz	−0.26	−0.10	−0.09

calculations are shown in the top panel of Fig. 9, which plots cumulative ΔI_{dB} as a function of stimulus level in %DR. For this exercise, calculations of consecutive ΔI_{dB} steps began at 0.5 dB SL and continued to the top of the dynamic range. For example, if the ΔI_{dB} at 0.5 dB SL was 2 dB then the next ΔI_{dB} was calculated at 2.5 dB SL, and so on. From these calculations, the number of consecutive discriminable intensity steps was counted for each subject. The resulting step counts are shown in the bar graph in the bottom panel of Fig. 9. A wide range of discriminable step counts was observed, from a low of 6.6 in DVS to a high of 45.2 in JPB.

Dynamic range varied considerably among subjects, but the sensitivity and slope of each subject's Weber function, and the dynamic range of the electrode in question, were all determinants of the total discriminable step count. For example, JWB had the widest dynamic range, but his Weber fractions were large at low levels so step size at low levels was large. The Weber function was moderately steep, so step size at higher levels was smaller, and the total step count reached 15 by the top of the dynamic range. Subject EES had better Weber fractions at low levels and a steep Weber function slope, but her dynamic range was so small that the total step count only reached 8.8. Subject RFM also had a small dynamic range, but his sensitivity was so good that the step count reached 35.7. Similar results were seen for JPB and FXC, whose step counts reached 45.2 and 29.2, respectively (the cumulative ΔI_{dB} curves for these subjects are not shown because they overlap with the curve for RFM). As indicated by the insert within the bottom panel of Fig. 9, the average number of discriminable intensity steps for normal acoustic hearing is 82.8. This estimate was calculated from parameters for the composite Weber functions reported by Schroder *et al.* (1994) at 300, 500, 1000, 2000, and 3000 Hz given in Table V. If the 30-dB dynamic range of speech were mapped into the top 30 dB of the acoustic dynamic range, the average number of discriminable steps would be 43.2, about the same number of steps available for JPB across his entire dynamic range.

In summary, the total number of discriminable intensity steps varied widely across subjects, more so than casual inspection of Weber fractions at a single level might suggest. The cumulative ΔI_{dB} curves in the top panel indicate that the discriminable step count is dependent upon overall sensitiv-

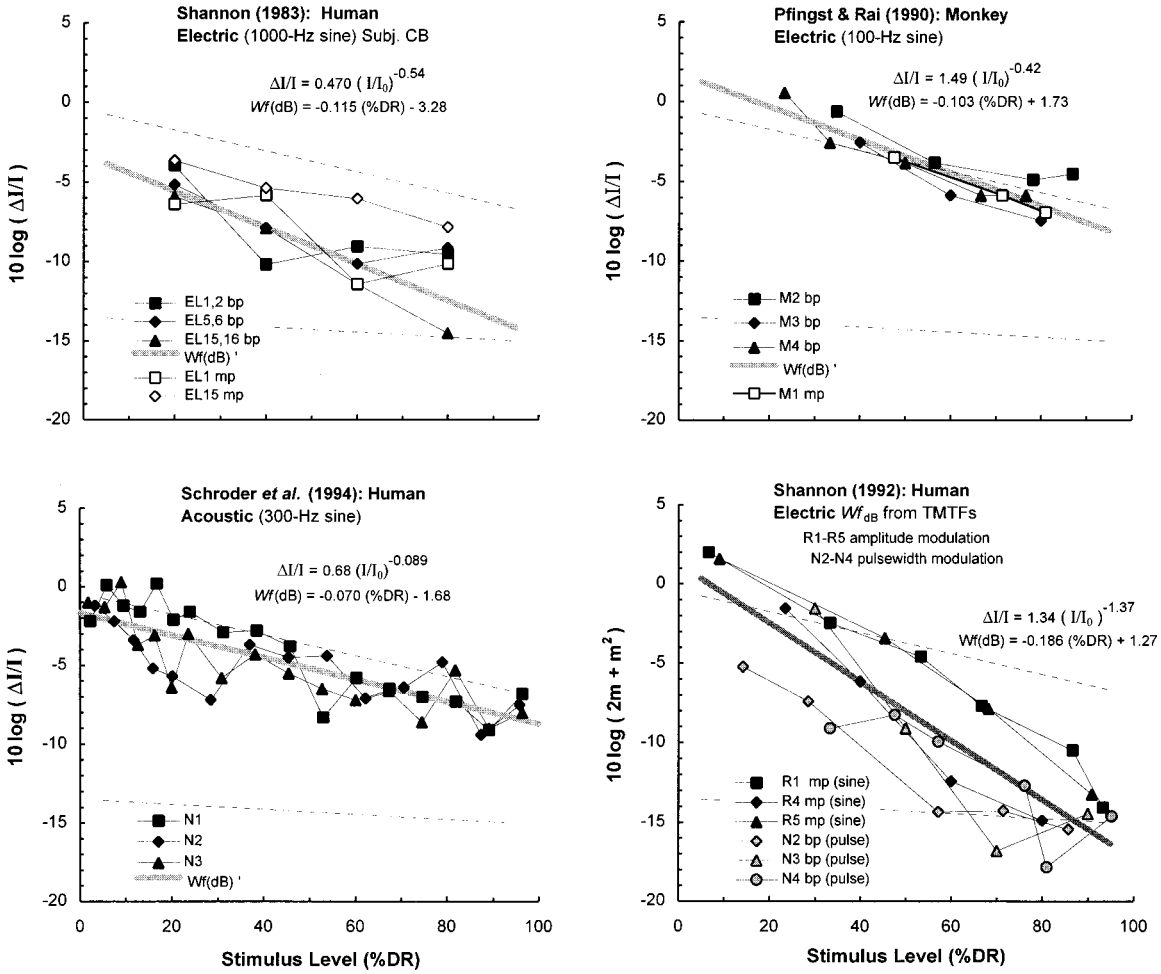

FIG. 10. Weber fractions in dB and composite Weber functions calculated for data from other investigations. The fitting parameters for Eq. (1) and Eq. (2) are shown within each panel. *Upper left panel*: Weber fractions calculated from data reported by Shannon (1983) for one cochlear implant subject (CB). Individual symbols indicate Weber fractions for different electrodes, labeled with electrode number and stimulation mode (bp—bipolar; mp—monopolar). A composite Weber function (heavy shaded line) was calculated from the mean fitting parameters for individual electrodes (bp electrodes only). *Upper right panel*: Weber fractions calculated from data reported by Pfingst and Rai (1990) from four monkeys. *Lower left panel*: Weber fractions from three human subjects reported by Schroder *et al.* (1994), replotted here as a function of percent dynamic range (%DR). *Lower right panel*: Weber fractions calculated from the most sensitive modulation-detection thresholds of temporal modulation transfer functions reported by Shannon (1992). Thin dashed lines in each panel are the composite Weber functions from subject DVS (top) and RFM (bottom), who demonstrated the worst and best Weber fractions, respectively, in the present study.

ity, the slope of the Weber function, and total dynamic range. This procedure for calculating resolvable intensity steps from subjects' composite Weber functions might prove useful in evaluating differences in subjects' speech discrimination abilities. The present data indicate that, in some subjects, the 30-dB dynamic range of speech is coded by fewer than seven discriminable intensity steps; in others, the number of discriminable intensity steps is close to the number of steps available in the top 30 dB of the normal acoustic dynamic range. Further research is needed to determine whether speech perception in some implant subjects is limited by a reduced number of discriminable intensity steps.

III. GENERAL DISCUSSION

A. Electric Weber fractions from other studies

The principal finding of this study is that electric intensity discrimination is well described by Weber fractions that improve systematically with stimulus intensity over the dynamic range. This finding is consistent with results from other investigations in humans and in monkeys. Shannon (1983) reported DLs for 100- and 1000-Hz sinusoids over the dynamic range of one cochlear implant subject (CB). His data for 1000-Hz sinusoids are replotted as Weber fractions in the upper-left panel of Fig. 10. Weber functions from the three bipolar electrodes tested were fitted with Eq. (2) and the fitting parameters are given in Table V. The composite Weber function (shaded line in Fig. 10) describes the trend across level for these three electrodes. Weber fractions improved with stimulus level and were not systematically different across electrodes. Slopes and intercepts for individual electrodes fell within the range seen in the present study. Shannon's subject CB exhibited Weber fractions that behaved very much like those seen in the present study, although they were not as sensitive as those obtained from our best subjects.[7]

Dillier *et al.* (1983) reported DLs for one electrode in each of two prelingually deafened subjects. They used 100-Hz, biphasic, 200-μs phase pulse trains presented at three stimulus levels throughout the dynamic range. For purposes of comparison, we converted their data to Weber fractions and fitted the resulting Weber functions with Eq. (2). The resulting fitting parameters are given in Table V. Subject RG demonstrated a Weber function with a steep slope and a moderate intercept, like many of the subjects in the present study. Subject EP's function had a flat slope and an extremely small intercept (-20.4), representing the smallest Weber fractions seen in any subject to date.

Busby *et al.* (1992) also measured DLs with 100-Hz trains of 200-μs phase biphasic pulses. They used a 4AFC adaptive procedure that estimated 50% correct intensity-decrement detection at a ''comfortable listening level'' on one electrode for each of ten prelingually deafened subjects. In addition, they measured psychometric functions for identification of level differences in three of those subjects. When we transformed their data into Weber fractions at a performance level of $d'=1.63$, the resulting Weber fractions ranged from -3.4 to -14.4 dB. This range is consistent with the Weber fractions obtained from subjects in the present study at 75% DR (see left panel of Fig. 7). Whereas Busby *et al.* did not specify the exact levels of their standard stimuli, it has been our experience that comfortable listening levels typically correspond to stimulus levels within the upper third of the dynamic range. Although the dynamic ranges of their subjects ranged from 2 to 16 dB, the correlation between dynamic range and Weber fractions was not significant ($p=0.5$). Absolute thresholds were not reported.

Shannon (1992) measured modulation transfer functions for electric stimulation using amplitude-modulated sinewaves or pulsewidth-modulated pulse trains as carrier stimuli. They reported the most sensitive modulation detection thresholds in terms of dB modulation ($20 \log m$, where m is the modulation depth) as a function of carrier level for seven implanted patients (their figure 4). The Weber fraction for modulated stimuli can be expressed in decibels as: $10 \log(\Delta I/I) = 10 \log(2m+m^2)$.[8] Weber fractions for six of Shannon's subjects are shown in the lower right panel of Fig. 10. Three subjects (R1, R4, R5) were tested with a modified method of limits procedure using amplitude-modulated sinewave carriers between 500 and 4000 Hz, and were stimulated with a monopolar electrode configuration. Another three subjects (N2, N3, N4) were tested with an adaptive 2AFC procedure using pulsewidth-modulated 100-μs/phase biphasic 1000-Hz pulse trains, and were stimulated with a bipolar electrode configuration. Weber functions were fit to each curve individually and the composite Weber function shown by the wide solid curve in Fig. 10 was calculated from the average slope and intercept across subjects; parameters for the composite Weber function are given in the figure. Note that Weber fractions derived from modulation detection thresholds exhibit the same intensity dependence observed here and in other studies using gated intensity increments. Weber functions are well described by a power function of intensity relative to absolute threshold. Exponents are somewhat larger than seen in the present study but sensitivity to intensity change falls in the same range. Sensitivity is slightly better for subjects N2–N5 than for subjects R1–R5. This could be due to differences in electrode configuration (bipolar versus monopolar) or to stimulus type (pulsatile versus sinusoidal), or could stem from the use of the more rigorous 2AFC psychophysical procedure with subjects N2–N5. The similarity between modulation-detection and increment-detection Weber functions suggests that the intensity dependence seen in temporal modulation transfer functions stems from the same underlying mechanisms that control the intensity dependence of Weber fractions. These mechanisms are discussed below.

Pfingst *et al.* (1983), Pfingst and Sutton (1983), and Pfingst and Rai (1990) reported intensity discrimination data from implanted monkeys, obtained with sinusoidal stimuli at several different frequencies. Data from four monkeys for 100-Hz sinusoids are replotted from Pfingst and Rai as Weber fractions in the upper right panel of Fig. 10. Again, Weber functions were fitted with Eq. (2) and the fitting parameters are given in Table V. The composite Weber function (wide shaded line) describes the trend across level exhibited on individual electrodes. Weber fractions improved with stimulus level and were not systematically different across electrodes. Slopes for individual monkeys fell within the range seen in the present study for humans, with an average slope of -0.10 that was just slightly steeper than the average slope of -0.08 reported here for humans. However, the intercepts were always higher for the monkey data (see Table V), indicating that the monkeys were less sensitive at all stimulus levels. This difference in the overall sensitivity to intensity change could stem from differences in the psychophysical tasks, or could reflect real interspecies differences. Alternatively, the poorer sensitivity to intensity change in monkeys could well stem from the use of stimuli with a longer effective charge duration: Shannon's (1983) DLs for 100-Hz sinusoids were slightly poorer than those for 1000-Hz sinusoids, Pfingst *et al.* (1983) reported poorer DLs for lower frequency sinewave stimuli, and White's (1984) single-pulse DLs in one subject were larger for 1800- than for 200-μs pulsewidths. Pfingst and Rai used 100-Hz sinusoids that are more like biphasic pulses with effective pulsewidths between 2000 and 5000 μs while the present study used biphasic pulses with 200-μs pulsewidths. This suggests that slopes of Weber functions might be similar for stimuli with short and long pulsewidths, but that DLs for longer pulsewidths would show poorer sensitivity overall.

In summary, studies evaluating intensity discrimination using biphasic pulses and sinusoids reveal a wide range of Weber functions. In most cases, Weber functions improve with stimulus level by 7 to 15 dB over the entire dynamic range. A few Weber functions do exhibit zero slopes, and those tend to occur in subjects who exhibit extremely small Weber fractions. With respect to the present data, it is interesting to note that subject AMA, who was prelingually deafened, and subject RFM, who was deafened later in life, both exhibited small Weber fractions. As mentioned above, other investigators have also reported sensitive DLs from prelingually deafened subjects. Thus in general, Weber fractions

for prelingually deafened subjects appear to be no better nor worse than those for other subjects.

B. Comparisons of electric and acoustic Weber fractions

Use of the Weber fraction in decibels as an index of intensity discrimination originated with studies of normal acoustic hearing. In Fig. 4, it was demonstrated that Weber fractions exhibit relatively constant variance across the dynamic range in electric hearing, as they do in acoustic hearing. On this basis, it can be argued that the Weber fraction is an appropriate metric for evaluating intensity discrimination as a function of stimulus level in electric hearing. In acoustic hearing, the Weber function is typically expressed in terms of the sensation level of the standard, as in Eq. (1). The bottom left panel in Fig. 10 demonstrates that acoustic Weber fractions can be described equally well by normalizing to dynamic range, as in Eq. (2).[9] Table V (bottom) shows the parameters of best fit obtained when Eq. (1) or Eq. (2) is applied to acoustic Weber fractions from Jesteadt *et al.* (1977) and Schroder *et al.* (1994). The parameters of best fit obtained with Eq. (1) or Eq. (2) are also shown in Table V for electric stimulation (top).

1. Intensity dependence

Consider first the exponents for acoustic and electric Weber functions. Equation (1), which expresses Weber functions in terms of dB SL, results in exponents (α) ranging from -0.07 to -0.11, averaging -0.09, for acoustic listeners. In contrast, exponents for cochlear implant listeners in the present study range from -0.27 to -3.21, averaging -1.3. Thus the average exponent for electric Weber functions, expressed in terms of dB SL, is at least ten times that for acoustic Weber functions. When the intensity dimension for acoustic data is normalized by dynamic range, as in Eq. (2), exponents (**a**) of Weber functions range from -0.06 to -0.10 across studies, and are similar to exponents obtained in electric hearing, which range from -0.02 to -0.15 across studies.

The similarity of Weber function exponents for electric and acoustic hearing, when both are normalized by the dynamic range, has some interesting implications. It suggests that the centrally based decision process must be similar for electric and acoustic intensity discrimination, and that the principal difference between acoustic and electric Weber fractions can be explained by an appropriate transformation of stimulus intensity. That transformation can be approximated by scaling the exponent in the power function of Eq. (1) by the ratio of the dynamic range for acoustic and electric hearing, as follows:

$$\alpha_{el} \cong \alpha_{ac}(DR_{ac}/DR_{el}). \quad (4)$$

Since the dynamic range in normal acoustic hearing is approximately ten times the average DR in electric hearing, Eq. (4) predicts that the exponent of the power function for electric intensity discrimination is approximately ten times the exponent for acoustic hearing. This implies that the intensity dimension in acoustic hearing is compressed by a 10:1 ratio compared to electric hearing.

The improvement with stimulus level for acoustic Weber fractions obtained with sinewaves has been referred to as the ''near miss'' to Weber's law (McGill and Goldberg, 1968). This departure from Weber's law is partially attributed to the steeper growth of response (e.g., discharge rate) with stimulus intensity in fibers best tuned to frequencies above the stimulus frequency and partially attributed to an increase in the number of neural fibers excited as stimulus level increases (Viemeister, 1988). Presumably, at least two physiological effects contribute to improvement in Weber fractions with stimulus intensity: Stimulation on the tails of high-frequency fibers results in steeper rate-intensity (RI) slopes for individual neurons (Evans, 1974; Abbas and Gorga, 1981; Harrison, 1981; Gorga and Abbas, 1981), which leads to a smaller DL for a rate-based detection criterion. More gradual (frequency rejection) slopes of neural tuning curves in their tail regions results in a faster spatial recruitment of contributing fibers with increased stimulus intensity (Evans, 1975). Both of these physiological factors, RI slopes and spatial recruitment, are likely to contribute to improved Weber fractions with stimulus level for acoustic stimulation. The nonlinear mechanisms that control these factors in the normal cochlea do not exist for electric stimulation. Thus different physiological mechanisms are needed to explain improvements in Weber fractions with stimulus level for electric stimulation. Such mechanisms must operate without the 10:1 intensity compression of acoustic hearing, and they must lead to steeper RI slopes and faster spatial recruitment of fibers as stimulus level is increased. Possible mechanisms are discussed below (Sec. III C).

2. Sensitivity to intensity changes

As indicated in Table V, sensitivity constants ($10 \log \beta$) for intensity discrimination in normal acoustic subjects range between $+0.60$ and -3.34 dB, depending on the study and test frequency. These values fall above and overlap with the upper range of sensitivity constants obtained with electric stimulation (-0.42 to -20.40). This suggests that Weber fractions are somewhat more sensitive in electric hearing than in acoustic hearing. Sensitivity differences in acoustic versus electric Weber fractions may stem from differences in the respective RI slopes of primary auditory neurons, although differences in spatial recruitment of fibers may also be involved at higher SLs. Slopes of RI functions for acoustically driven auditory-nerve fibers are inversely proportional to fiber dynamic range (DR), with DR expressed as the dB difference in stimulus intensities producing 10% and 90% of maximum driven response. These slopes are well-described by a unit-less quantity equal to 38.5/DR (Sachs and Abbas, 1974). Slopes computed from fiber spontaneous rate, fiber maximal firing rate, and stimulus intensity, average 1.98 for acoustically driven fibers (Javel, 1996); the DR corresponding to this mean slope is 19.4 dB (38.5/1.98). Slopes of RI functions for electrically driven fibers depend upon several factors, including stimulus presentation rate, pulsewidth, and degree of neural degeneration. For 100-μs/phase biphasic stimuli presented at 200 Hz, RI slopes for electrical stimulation average about 26 in short-term deafened animals (Javel,

unpublished). Thus slopes for electrical stimulation are around 13 times steeper than the average slope of 1.98 for acoustically driven fibers.

Again, the absence of cochlear preprocessing may be the primary determinant of steeper RI functions for electrical stimulation. The magnitude of the difference in RI slopes for acoustic and electric stimulation is consistent with average sensitivity constants ($10 \log \beta$) for electric stimulation reported here, which are about an order of magnitude better than for acoustical stimulation (see Table V). If intensity discrimination is based upon spike counts (or firing rate), then the steeper RI functions in electric hearing can, in general, account for the smaller Weber fractions observed here.[10]

This comparison between Weber-function parameters for electric and acoustic listeners suggests the following three generalizations: First, Weber functions obtained with electric and acoustic stimulation are well described by the same power function of stimulus sensation level given by Eq. (1). Second, the exponent of the power function (α) for electric Weber functions is, on average, an order of magnitude larger than that for acoustic Weber functions, probably because the normal cochlear-based intensity compression is absent in electric hearing. Third, sensitivity to intensity changes appears to be better for electric stimulation, at least partly because RI functions for individual neurons are steeper in the electric case.

C. Physiological mechanisms behind individual differences

Viemeister (1988) demonstrated that a rate-based neural code, or neural count model, can account for the overall sensitivity to intensity change under acoustic stimulation. His analysis of neural firing rates in acoustically driven fibers suggests that excellent sensitivity to intensity change can be traced to response statistics of auditory neurons. Such a neural count model assumes that the neural response to an incremented stimulus exceeds the response to a standard stimulus by some criterion. It also assumes that the decision statistic for this rate code is mediated central to the cochlea, which is likely to be the case for electrical stimulation as well. If so, then major differences between acoustic and electric Weber functions should stem from differences in cochlear preprocessing. As previously stated, those differences are characterized by a 10:1 difference in Weber-function exponents and a difference in overall sensitivity to intensity change. Both may be explained by the existence of cochlear preprocessing (intensity compression) in the acoustic case only. Since cochlear preprocessing is absent in the electric case, individual differences in intensity discrimination ability among cochlear implant subjects must stem primarily from differences in neural function. We will focus on such individual differences in the discussion that follows.

The criterion increase in neural spike count necessary to achieve increment detection in a neural count model can occur in one of two ways: (1) by increasing the average firing rate in a fixed set of auditory-nerve fibers, or (2) by increasing the number of fibers responding as intensity is incremented. To explain differences among cochlear implant subjects, one must look to physiological mechanisms that incorporate one or both of these factors.

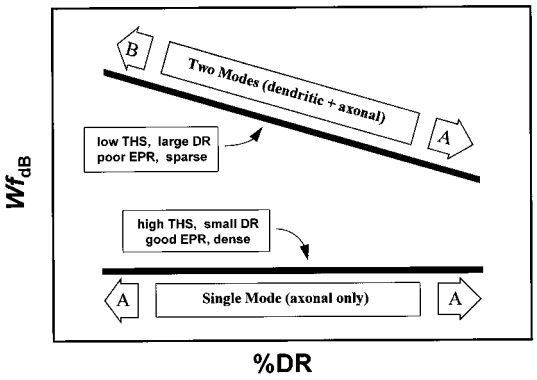

FIG. 11. Rate-based qualitative model of electric Weber fractions, incorporating different modes of neural excitation and different patterns of neural survival. The two solid curves represent Weber functions that encompass the two extremes of Weber functions observed for electric stimulation. For the upper curve, two modes of neural excitation, dendritic (type **B**) and axonal (type **A**), are presumed to contribute to intensity discrimination (indicated by the shaded arrows): Dendritic stimulation with more gradual rate-intensity functions predominates at low levels; axonal stimulation with steep rate-intensity functions predominates at high levels. Other factors associated with the upper curve (upper inset) include: low absolute threshold (THS), large dynamic range (DR), poor electrode pitch ranking (EPR) for comfortably loud stimuli, and presumably sparse axonal survival because electrode pitch ranking is poor. For the lower curve, a single mode of neural excitation is presumed to contribute to intensity discrimination (indicated by the shaded arrows): Axonal stimulation near cell bodies within the modiolus leads to steep rate-intensity functions at all stimulus levels. Other factors associated with the lower curve (lower inset) include: high absolute threshold, small dynamic range, good electrode pitch ranking, and presumably dense axonal survival because electrode pitch ranking is good for comfortably loud stimuli.

As described earlier, Weber functions normalized to dynamic range for electric hearing tend to fall between two extremes. Those two extremes are illustrated by the solid curves in Fig. 11. The uppermost, negatively sloped, Weber function represents poor Weber fractions at low intensities, which improve dramatically over the dynamic range. As indicated within the upper inset, other factors associated with this extreme were low absolute thresholds, large dynamic ranges and poor pitch ranking. The lower, flat-sloped, Weber function represents excellent Weber fractions, which remain relatively constant over the entire dynamic range. As indicated within the lower inset, other factors associated with this extreme were high absolute thresholds, small dynamic ranges and good pitch ranking. In order for a rate-based intensity code to explain electric intensity discrimination, physiological mechanisms that differentially affect neural growth rates must be identified, and those mechanisms must account for Weber functions ranging between the two extremes shown in Fig. 11.

1. Two modes of neural excitation: Dendritic and axonal

One such physiologic mechanism involves the existence of two modes of neural excitation. One mode of excitation produces more gradual rate-intensity functions, operates at lower stimulus levels than the other, and can be associated

with different neural survival characteristics. Specifically, Van den Honert and Stypulkowski (1984), Javel (1990), and Javel *et al.* (1991) have reported different types of neural responses to intracochlear electric stimulation of auditory-nerve fibers. Each has a characteristic latency and rate of response growth, and is associated with a specific mode of neural excitation. At low stimulus levels a **B** response, with a long latency (0.7 ms) and gradual rate of response growth, predominates. This response is thought to be associated with neural excitation from unmyelinated peripheral processes that have long time constants (*dendritic* stimulation). At higher stimulus levels an **A** response, with a shorter latency ($<$0.5 ms) and a very steep growth rate, predominates. This response has been associated with direct excitation of the fiber near the cell body and a short neural time constant (*axonal* stimulation). In the population neural response, these two level-dependent modes of neural excitation coexist. The mode with the more gradual growth rate, associated with dendritic stimulation, may predominate for low-level stimulation near absolute threshold; the mode with the steeper growth rate, associated with axonal stimulation, may predominate at high stimulus levels; both modes may contribute to neural growth rates at moderate stimulus levels.[11]

2. Qualitative model of intensity discrimination

The shaded insets and arrows in Fig. 11 illustrate how the existence of level-dependent dendritic and axonal excitation might contribute to rate-based explanations of electric intensity discrimination. The upper, negatively sloped, Weber function represents the case where intact auditory fibers with some functional unmyelinated peripheral processes presumably exist. Larger Weber fractions occur at low stimulus levels where type **B** (dendritic) responses and gradual rate-intensity functions predominate. Smaller Weber fractions occur at high levels where type **A** (axonal) responses and steep rate-intensity functions predominate. This pattern was observed in the present study for several subjects whose absolute thresholds were low and dynamic ranges were large (e.g., JWB). In these cases, it is reasonable to theorize the survival of substantial numbers of spiral ganglion cells with some intact peripheral processes that exhibit relatively long time constants. This assumption predicts low absolute thresholds (and wide dynamic ranges), since unmyelinated peripheral processes exist in close proximity to the bipolar stimulating electrodes, and, in addition, their longer time constants may integrate current over time to achieve sensitive absolute thresholds.

Several other cochlear implant subjects (e.g., RFM) exhibited extremely small Weber fractions with little intensity dependence, as illustrated by the lower solid curve in Fig. 11. The same qualitative model described above should account for this pattern. In this case, dendritic processes may be absent near the stimulating electrodes, and consequently, excitation is primarily axonal (modiolar) at both low and high stimulus levels. Absolute thresholds are high because the axonal targets are distant from the stimulating electrodes and their shorter time constants may not be conducive to integrating low currents over time. Related to this, dynamic ranges are narrow because stimulus levels only slightly above threshold result in simultaneous excitation of many neurons at their proximal processes. Rate-intensity functions are steep at all stimulus levels, due to the predominance of axonal excitation sites. A small increase in intensity produces a relatively large increment in the total spike count; thus the criterion increase needed for increment detection is achieved with only a small stimulus change. Consequently, Weber fractions are small throughout the dynamic range and do not improve significantly with level.

The simple model just described, which incorporates two modes of neural excitation and variable patterns of neural survival, accounts qualitatively for the range of Weber functions revealed here. Given this, Weber-function patterns might be useful as an index of neural morphology in individual subjects. Of course, caution should be exercised in drawing conclusions about underlying neural status from Weber fractions, since very limited morphologic data are available for animals in which psychophysical measures have also been obtained. However, those data that do exist are encouraging. In monkeys, Pfingst *et al.* (1983) found that intensity discrimination was poorer in two cochleas showing relatively little pathology, as compared to three cochleas showing more severe pathology but better intensity discrimination. Indices reported were spiral ganglion cell counts and observations of myelinated nerve fibers (axons), thus, direct inferences related to dendritic survival cannot be made from their work. However, it seems likely that some peripheral processes might have been present in the two cochleas with the least pathology. If so, then the findings reported by Pfingst *et al.* are consistent with the qualitative model offered here.

3. Contributions of neural density and spatial spread of current

In addition to physiological factors that modify firing rates in individual nerve fibers, one must also consider how the spatial spread of current might recruit additional fibers. This is necessary because the dynamic range over which intensity discrimination can be measured is considerably larger than the dynamic range of individual fibers. At low pulse rates ($<$200 Hz), fibers that respond near absolute threshold saturate within a few decibels above threshold. To maintain the intensity code with increasing level, these saturated fibers must be supplemented by unsaturated fibers. Unsaturated fibers may be recruited at the edge of the spatial excitation pattern as intensity increases, or they may be recruited by current flowing into the modiolus and producing global activation of fibers.

For the case where the Weber function is similar to that shown by the upper curve in Fig. 11, we have postulated some survival of peripheral processes. As stimulus intensity increases above threshold, new fibers are recruited at a gradual rate because the density of peripheral processes is presumed to be relatively low. As a result of relatively shallow rate-intensity functions and gradual rates of fiber recruitment, the increase in total spike count associated with a fixed increment in intensity is small. Thus relatively large increments in stimulus intensity are needed to reach a criterion increase in spike count for increment detection. This trans-

lates to large Weber fractions. As stimulus intensity increases to moderate and high stimulus levels, the current field expands to encompass more peripheral processes along a wider extent of the cochlear partition, but *more importantly,* fibers nearest the electrode become stimulated at their central (axonal) processes. Not only are rate-intensity functions steeper for axonal stimulation, but neural density is probably higher in the modiolus. These two factors (steeper RI slopes and higher neural density) may combine to generate rapid growth in overall response with stimulus level, and a smaller intensity increment is required to achieve a criterion increase in spike count. The result is smaller Weber fractions. In this way, Weber fractions that are relatively large near absolute threshold, may decrease substantially as level increases over the dynamic range.

4. Electrode pitch ranking and intensity discrimination

The strong positive correlation between electrode pitch ranking and intensity discrimination (Table IV) also seems consistent with the qualitative model depicted in Fig. 11. Excellent electrode pitch ranking for comfortably loud stimuli was exhibited by subjects whose Weber functions approached the bottom curve, i.e., highly sensitive and flat Weber functions accompanied by high absolute thresholds and small dynamic ranges. Although little is known about the physiological mechanisms underlying good pitch ranking, the demonstration of excellent pitch ranking (and excellent electrode discrimination) suggests to us that the underlying fiber population must be dense and probably tonotopically organized. Furthermore, the fact that the electrode pitch ranking experiment was carried out with stimuli in the upper third of the dynamic range, probably indicates that the stimulated fiber population was primarily axonal. As argued earlier, small Weber fractions at low sensation levels suggest that axonal stimulation is primarily involved. Thus both excellent pitch ranking and excellent intensity discrimination are consistent with good survival of cell bodies within the modiolus.

At the other extreme, poor electrode pitch ranking was exhibited by subjects whose Weber functions approached the top curve in Fig. 11, i.e., less sensitive and steeply sloped Weber functions, accompanied by low absolute thresholds and large dynamic ranges. As argued earlier, larger Weber fractions at low intensities suggests that dendritic stimulation was involved. Poor pitch ranking ability for comfortably loud stimuli suggests that the underlying axonal population was relatively sparse and perhaps patchy throughout the cochlea. These outcomes are consistent with our qualitative model: The longer time constants (or closer proximity to the stimulating electrodes) of dendritic processes resulted in lower absolute thresholds, and the gradual RI functions associated with dendritic stimulation were responsible for poorer Weber fractions at low intensities. At intensities near the top of the dynamic range, axonal stimulation predominated, and Weber fractions improved. However, the slightly poorer Weber fractions seen at high intensities in these subjects may reflect the somewhat poorer ganglion cell survival that we have associated with poorer electrode pitch ranking.

The relationship between differential sensitivity to intensity change and neural survival characteristics is clearly complex. We have offered a simple qualitative model that, to a first approximation, can account for large individual differences in intensity discrimination and electrode pitch ranking by invoking two modes of neural excitation and differential patterns of neural survival. However attractive this simple model might seem, it is still largely speculative. Clearly, additional research is needed to establish relevant links between morphology, physiology, and behavior in animal subjects. Knowledge from such studies may permit a confident understanding of individual subject differences, which can then be applied to the design of optimized processing schemes for individual implant users.

IV. CONCLUSIONS

(1) Intensity discrimination of 200-μs/phase biphasic electric pulses can be accurately quantified by Weber fractions in decibels $\{10 \log(\Delta I/I)\}$, which improve as a power function of stimulus intensity relative to absolute threshold $\{\Delta I/I = \beta(I/I_0)^{\alpha}\}$, just as they do for acoustic stimulation. The exponents of electric Weber functions vary between -0.4 and -3.2, compared to exponents between -0.07 and -0.11 for acoustic stimulation. The average Weber-function exponent for electric stimulation is an order of magnitude larger than the average exponent for acoustic stimulation. This probably reflects the absence of nonlinear cochlear preprocessing, which results in a nearly linear intensity dimension for electric stimulation.

(2) Normalization of Weber-function exponents to the dynamic range of hearing $\{\alpha(\mathrm{DR}/100)\}$ equalizes improvements in Weber fractions with stimulus intensity, both for acoustic versus electric stimulation, and for electrodes with disparate dynamic ranges. The average improvement in Weber fractions over the dynamic range is approximately 8 dB, for both acoustic and electric stimulation. This suggests that centrally based decision mechanisms are probably the same but that the peripheral transformations of stimulus intensity are quite different for acoustic and electric stimulation.

(3) Overall sensitivity to intensity change $\{10 \log \beta\}$ is better for electric stimulation than for acoustic stimulation. This probably reflects steeper neural rate-intensity functions for electrical stimulation.

(4) Some subjects who exhibit very small Weber fractions also exhibit little change in sensitivity across the dynamic range, or across portions of the dynamic range. In many cases, constant Weber fractions occur because the intensity resolution of implanted receiver/stimulators prohibits measurement of smaller Weber fractions.

(5) Forced choice adaptive procedures yield electric Weber fractions that are consistent with those obtained from fixed-level procedures. Fixed-level procedures demonstrate that psychometric functions for intensity discrimination are monotonic and that d' is a linear function of ΔI.

(6) Weber fraction variance for electric stimulation is constant with stimulus level, just as it is for normal acoustic hearing.

(7) Weber fractions from prelingually deafened subjects

appear no better or worse than those from postlingually deafened subjects.

(8) The cumulative number of discriminable intensity steps across the dynamic range of electric hearing varies considerably among subjects, from as few as 6.6 to as many as 45.2 steps, depending upon dynamic range, overall sensitivity to intensity increments, and rate of improvement of the Weber fraction with stimulus level.

(9) DLs, expressed as amplitude increments (ΔA), were not constant across dynamic range.

(10) Intensity discrimination was related to absolute threshold, dynamic range, and electrode pitch ranking. Subjects with larger Weber fractions exhibited lower absolute thresholds, wider dynamic ranges, and poorer electrode pitch ranking. A qualitative model associates this pattern with more gradual neural rate-intensity functions and sparse dendritic survival. Subjects with excellent Weber fractions exhibited high absolute thresholds, small dynamic ranges, and excellent electrode pitch ranking. The model associates this pattern with steep neural rate-intensity functions and dense axonal survival.

ACKNOWLEDGMENTS

This work was supported by Grant No. DC00110 from NIDCD and by the Lions 5M International Hearing Foundation. John Van Essen converted Robert Shannon's computer software into the C language and made modifications to that software. Leigha Jansen and Anna Schroder provided valuable assistance during data collection and analysis. Robert Schlauch, Anna Schroder, Robert Shannon, Fan-Gang Zeng, and an anonymous reviewer provided valuable comments on earlier versions of this manuscript. Portions of this work were submitted to the Graduate School of the University of Minnesota as a Master's thesis in Communication Disorders by Jennifer L. (Kujala) Schmitz.

[1]Electrodes are identified by their numbers with the prefix rEL before the number. This is to remind the reader (and the authors) that the numbering scheme is that used for research (apex-to-base) as opposed to the numbering scheme used by Cochlear Corp. for clinical mapping (base-to-apex).

[2]A CSU is the smallest change in current realizable with the implanted stimulator. The exact decibel step size corresponding to one CSU varies slightly across the dynamic range and among individual implanted stimulators, but is usually between 0.1 and 0.2 dB.

[3]Data were examined using other indices of dynamic range as well, such as $(I-I_0)/(I_M-I_0)\cdot 100$ and $(A-A_0)/(A_M-A_0)\cdot 100$. The primary effect of using these indices was a reduction in the intercept of the Weber function, with a slight steepening of the slope. The reduction in intercept was larger for larger dynamic ranges. However, the general form of the Weber function was maintained regardless of the index of dynamic range employed.

[4]Because RFM's adaptive Weber fractions were clearly at the intensity resolution limits of the stimulator, Weber fractions obtained from psychometric functions were used in later analyses. Note also that the adaptive Weber fractions around 80%DR for RFM were all better than 0.5 CSUs and, therefore, are not plotted in Fig. 3.

[5]Weber fractions for all electrodes tested in subject DVS were derived from psychometric functions and were supported by multiple retests using the adaptive procedure.

[6]Transformations of Weber functions with negative slopes into corresponding amplitude DL curves will result in amplitude DL curves with slopes ranging from negative to positive. For example, a Weber function with a slope of -0.06, an intercept of -3.2 dB and a dynamic range of 10 dB will transform into an amplitude DL curve with a slope of $+0.00$ and an intercept of 10.1%DR, which will appear as a constant amplitude DL across the dynamic range. Changing the Weber function slope to -0.05 yields an amplitude DL curve with a slope of $+0.02$, which will appear as a worsening amplitude DL across the dynamic range. Thus Weber functions that vary across a range of negative slopes, as seen in the present data, will appear differently when viewed as amplitude DL curves.

[7]Shannon's 2AFC psychophysical procedure tracked 70.7% correct, which estimates a performance level of $d'=0.78$, while the 3AFC procedure in the current study tracked 79.4% correct, which estimates a performance level of $d'=1.63$. Therefore, Weber fractions calculated from Shannon's data should be corrected by $+3.2$ dB $\{10\log(1.63/0.78)\}$ to conform to those obtained in the present study. Such a correction would yield an intercept of -0.08 instead of -3.28 for the composite Weber function in the upper left panel of Fig. 10.

[8]One can derive DLs from modulation detection thresholds, if one assumes that a Weber fraction $(\Delta I/I)$ is equivalent to: $(I(1+m)^2-I)/I=2m+m^2$. Then the Weber fraction in decibels becomes

$$10\log(\Delta I/I)=10\log(2m+m^2).$$

[9]For the acoustic data from Schroder *et al.* (1994), estimates of maximum acceptable loudness (MAL) levels were not available. Thus to approximate dynamic ranges for acoustic stimulation, an MAL at 100 dB SPL was assumed for all test frequencies, and dynamic range was specified as the difference in dB between MAL and mean absolute threshold for their subjects at each test frequency.

[10]For the purposes of this discussion, differences in the underlying variance of the distribution of spike counts has been ignored. Any realistic spike-count model must take this into account; unfortunately, neurophysiological data are lacking in this regard.

[11]This reasoning assumes some dendritic survival, which might not always be the case. However, it also applies to the ''shrunken axon'' case where long-term degeneration has led to complete loss of peripheral processes and reduced fiber diameters. This latter situation has been observed (Javel, unpublished) but is not yet well documented. Shrunken axons would be expected to generate neural responses with high thresholds and gradual rates of response growth.

Abbas, P. J., and Gorga, M. P. (**1981**). ''AP responses in forward-masking paradigms and their relationship to responses of auditory-nerve fibers,'' J. Acoust. Soc. Am. **69**, 492–499.

Aran, J. M. (**1981**). ''Electrical stimulation of the auditory system and tinnitus control,'' J. Laryngol. **4**, 153–162.

Busby, P. A., Tong, Y. C., and Clark, G. M. (**1992**). ''Psychophysical studies using a multiple-electrode cochlear implant in patients who were deafened early in life,'' Audiology **31**, 95–111.

Dillier, N., Spillmann, T., and Guntensperger, J. (**1983**). ''Computerized testing of signal encoding strategies with round window implants,'' in *Cochlear Prostheses: An International Symposium*, edited by C. W. Parkins and S. W. Anderson (Ann. N.Y. Acad. Sci., New York), Vol. 405, pp. 360–369.

Douek, E., Fourcin, A. J., Moore, B. C. J., and Clark, G. P. (**1977**). ''A new approach to the cochlear implant,'' Proc. R. Soc. Med. **70**, 379–383.

Eddington, D. K., Doebelle, W. H., Brackmann, D. E., Mladejovsky, M. G., and Parkin, J. L. (**1978**). ''Auditory prostheses research with multiple channel intracochlear stimulation in man,'' Ann. Otol. **87**, 1–39.

Evans, E. F. (**1974**). ''Auditory frequency selectivity and the cochlear nerve,'' in *Facts and Models in Hearing*, edited by E. Zwicker and E. Terhardt (Springer-Verlag, Berlin), pp. 118–129.

Evans, E. F. (**1975**). ''The sharpening of cochlear frequency selectivity in the normal and abnormal cochlea,'' Audiology **14**, 419–442.

Fourcin, A. J., Rosen, S. M., Moore, B. C. J., Douek, E. E., Clarke, G. P., Dodson, H., and Bannister, L. H. (**1979**). ''External electrical stimulation of the cochlea: Clinical, psychophysical, speech perceptual and histological findings,'' Br. J. Audiol. **13**, 85–107.

Gorga, M. P., and Abbas, P. J. (**1981**). ''Forward-masking AP tuning curves in normal and in acoustically traumatized ears,'' J. Acoust. Soc. Am. **70**, 1322–1330.

Hacker, M. J., and Ratcliff, R. (**1979**). ''A revised table of d' for M-alternative forced choice,'' Percep. Psychophys. **26**, 168–170.

Harrison, R. V. (**1981**). ''Rate-versus-intensity functions and related AP responses in normal and pathological guinea pig and human cochleas,'' J. Acoust. Soc. Am. **70**, 1036–1044.

Hochmair-Desoyer, I. J., Hochmair, E. S., Burian, K., and Fisher, R. E. (**1981**). ''Four years of experience with cochlear prostheses,'' Med. Progr. Technol. **8**, 107–119.

Hochmair-Desoyer, I. J., Hochmair, E. S., Burian, K., and Stiglbrunner, H. K. (**1983**). ''Percepts from the Vienna cochlear prostheses,'' in *Cochlear Prostheses: An International Symposium*, edited by C. W. Parkins and S. W. Anderson (Ann. N.Y. Acad. Sci., New York), Vol. 405, pp. 295–306.

House, W. F., and Edgerton, B. J. (**1982**). ''A multiple-electrode cochlear implant,'' Ann. Otol. Rhinol. Laryngol. **91**, 104–116.

Javel, E. (**1990**). ''Acoustic and electrical encoding of temporal information,'' in *Cochlear Implants: Models of the Electrically Stimulated Ear*, edited by J. M. Miller and F. A. Spelman (Springer-Verlag, New York), pp. 247–295.

Javel, E. (**1996**). ''Excitation pattern model of the cat auditory nerve with interfiber variability and stochastic response properties. I. Analysis of fiber responses and development of the model'' (submitted).

Javel, E., White, M. W., Finley, C. C., and Shepherd, R. K. (**1991**). ''Validation of a stochastic model of electrically excited auditory nerve fibers,'' ARO Abstracts **14**, 130.

Jesteadt, W., Wier, C. C., and Green, D. M. (**1977**). ''Intensity discrimination as a function of frequency and sensation level,'' J. Acoust. Soc. Am. **61**, 169–177.

Levitt, H. (**1971**). ''Transformed up–down methods in psychoacoustics,'' J. Acoust. Soc. Am. **49**, 467–477.

McGill, W. J., and Goldberg, J. P. (**1968**). ''A study of the near miss involving Weber's law and pure-tone intensity discrimination,'' Percep. Psychophys. **4**, 105–109.

Nelson, D. A., Van Tasell, D. J., Schroder, A. C., Soli, S., and Levine, S. (**1995**). ''Electrode ranking of ''place pitch'' and speech recognition in electrical hearing,'' J. Acoust. Soc. Am. **98**, 1987–1999.

Pfingst, B. E. (**1984**). ''Operating ranges and intensity psychophysics for cochlear implants. Implications for speech processing strategies,'' Arch. Otolaryngol. **110**, 140–144.

Pfingst, B. E. (**1988**). ''Comparisons of psychophysical and neurophysiological studies of cochlear implants,'' Hear. Res. **34**, 243–251.

Pfingst, B. E., and Rai, D. T. (**1990**). ''Effects of level on nonspectral frequency difference limens for electrical and acoustic stimuli,'' Hear. Res. **50**, 43–56.

Pfingst, B. E., and Sutton, D. (**1983**). ''Relation of cochlear implant function to histopathology in monkeys,'' Ann. N.Y. Acad. Sci. **405**, 224–239.

Pfingst, B. E., Burnett, P. A., and Sutton, D. (**1983**). ''Intensity discrimination with cochlear implants,'' J. Acoust. Soc. Am. **73**, 1283–1292.

Sachs, M. B., and Abbas, P. J. (**1974**). ''Rate versus level functions for auditory-nerve fibers in cats: Tone-burst stimuli,'' J. Acoust. Soc. Am. **56**, 1835–1847.

Schroder, A. C., Viemeister, N. F., and Nelson, D. A. (**1994**). ''Intensity discrimination in normal-hearing and hearing-impaired listeners,'' J. Acoust. Soc. Am. **96**, 2683–2693.

Shannon, R. V. (**1983**). ''Multichannel electrical stimulation of the auditory nerve in man. I. Basic psychophysics,'' Hear. Res. **11**, 157–189.

Shannon, R. V. (**1992**). ''Temporal modulation transfer functions in patients with cochlear implants,'' J. Acoust. Soc. Am. **91**, 2156–2163.

Shannon, R. V., Adams, D. D., Ferrel, R. L., Palumbo, R. L., and Grandgenett, M. (**1990**). ''A computer interface for psychophysical and speech research with the Nucleus cochlear implant,'' J. Acoust. Soc. Am. **87**, 905–907.

Simmons, F. B. (**1966**). ''Electrical stimulation of the auditory nerve in Man,'' Arch. Otolaryngol. **84**, 24–76.

Tong, Y. C., Busby, P. A., and Clark, G. M. (**1988**). ''Perceptual studies on cochlear implant patients with early onset of profound hearing impairment prior to normal development of auditory, speech, and language skills,'' J. Acoust. Soc. Am. **84**, 951–962.

van den Honert, C., and Stypulkowski, P. H. (**1984**). ''Physiological properties of the electrically stimulated auditory nerve. II. Single fiber recordings,'' Hear. Res. **14**, 225–243.

Van Tasell, D. J., Greenfield, D. G., Logeman, J. L., and Nelson, D. A. (**1992**). ''Temporal cues for consonant recognition: training, talker generalization, and the use in evaluation of cochlear implants,'' J. Acoust. Soc. Am. **92**, 1247–1257.

Viemeister, N. F. (**1988**). ''Psychophysical aspects of auditory intensity coding,'' in *The Auditory System: Development, Physiology, and Psychophysics*, edited by G. M. Edelman, W. E. Gall, and W. M. Cowan (Wiley, New York), pp. 213–241.

White, M. W. (**1984**). ''Psychophysical and neurophysiological considerations in the design of a cochlear prosthesis,'' Audiol. Ital. **1**, 77–117.